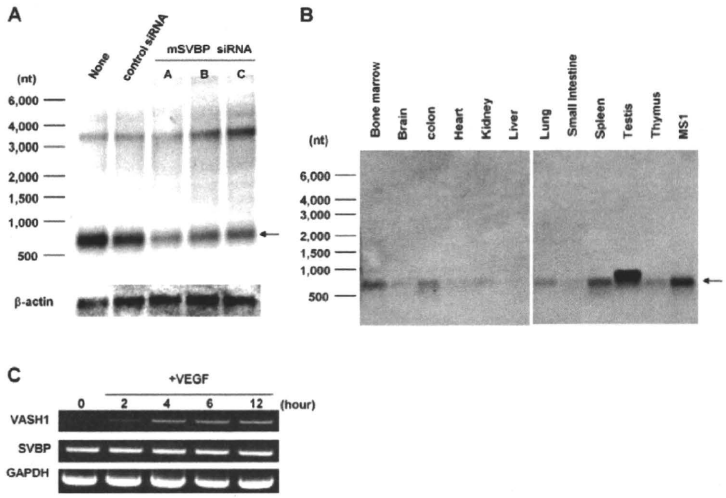

Fig. 2. In vitro and in vivo expression of *Svbp* and *Vash1* mRNA. (**A**) MS1 cells were transiently transfected with three different siRNAs designed for mouse ***Svbp*** mRNA and the expression evaluated by Northern blot. β-actin was used as an internal control. (**B**) ***Svbp*** mRNA (arrow) was extracted from the indicated adult mouse organs and analyzed by Northern blot. (**C**) MS1 cells pre-incubated in 0.1% FBS in α-MEM for 12 hours were stimulated with 20 ng/ml VEGF for the indicated periods. RT-PCR was performed on total RNA using specific primer pairs for mouse VASH1, SVBP and glyceraldehyde 3-phosphate dehydrogenase (GAPDH).

of VASH1 and SVBP in relation to cell polarity (Sabath et al., 2008). We confirmed that the tight junction marker ZO-1 was present at the apical side of MDCK cells (Fig. 4C). When VASH1 and SVBP cDNAs were co-transfected into MDCK cells, SVBP localized mainly on the apical side. This apical localization coincided with ZO-1. By contrast, VASH1 was present throughout the cell and partially colocalized with SVBP on the apical side (Fig. 4D). Positive signals of PLA were observed in the apical side of MDCK cells co-transfected with VASH1 and SVBP expression vectors (Fig. 4E), indicating that SVBP and VASH1 binds and colocalizes in the apical side of cells.

SVBP enhances VASH1 solubility and secretion

A previous report showed that VASH1 does not contain any classical signal sequence for translocation to the ER and does not colocalize with the ER marker calnexin (Watanabe et al., 2004). The above evidence that SVBP interacts with VASH1 both intracellularly and extracellularly prompted us to evaluate whether SVBP might affect VASH1 secretion. We transfected equal amounts of VASH1 expression vector and increasing amounts of SVBP expression vector into MS1 cells and found that SVBP enhanced the secretion of VASH1 in a dose-dependent manner (Fig. 5A). This increased secretion of VASH1 by SVBP was confirmed by ELISA, which measured the concentration of the VASH1–SVBP complex (Fig. 5B). Moreover, we confirmed that Brefeldin A, an inhibitor of ER- and Golgi-dependent secretory transport (Nickel, 2007; Seelenmeyer et al., 2003), does not affect the secretion of VASH1 (Fig. 5B), suggesting that VASH1 might be released from ECs via an unconventional secretion pathway (Nickel and Rabouille, 2009). We also observed that SVBP enhanced the secretion of VASH2, which also lacks a signal sequence (Fig. 5C). Furthermore, the interaction between VASH1 and SVBP dramatically changed the ability to extract VASH1 protein into 1% Triton X-100 cell lysis buffer (Fig. 5A). SVBP increased the amount of VASH1 in the soluble fraction, which coincided with a decrease of VASH1 in the insoluble fraction. The solubility of β-actin, an internal control, was not affected by SVBP. When endogenous SVBP was knocked down by siRNA, we observed the

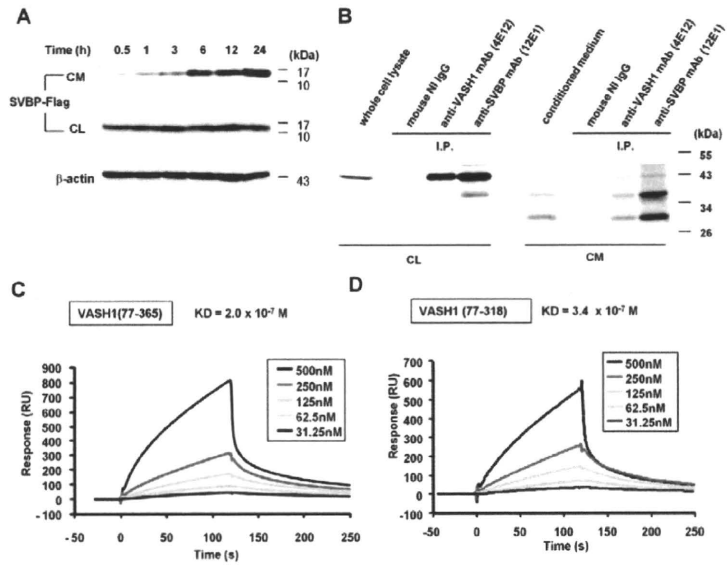

Fig. 3. SVBP–VASH1 complexes in the cell lysate and CM. (**A**) Time-course of SVBP release from ECs. MS1 cells transiently transfected with p3xFLAG-SVBP for 24 hours were washed with serum-free α-MEM, and then cultured in 0.1% FBS in α-MEM for the indicated periods. Concentrated CM and Cell lysate (CL) were evaluated by western blot. (**B**) Co-immunoprecipitation of the SVBP–VASH1 protein complex from HUVECs. CL from confluent HUVECs and their CM were immunoprecipitated with either anti-human VASH1 antibody or anti-human SVBP antibody as indicated. Immunoprecipitates were analyzed by western blot analysis using peroxidase-conjugated anti-human VASH1 antibody. IP, immunoprecipitation. (**C**,**D**) Kinetic analysis of the direct binding between SVBP and truncated forms of VASH1 using the BIAcore system.

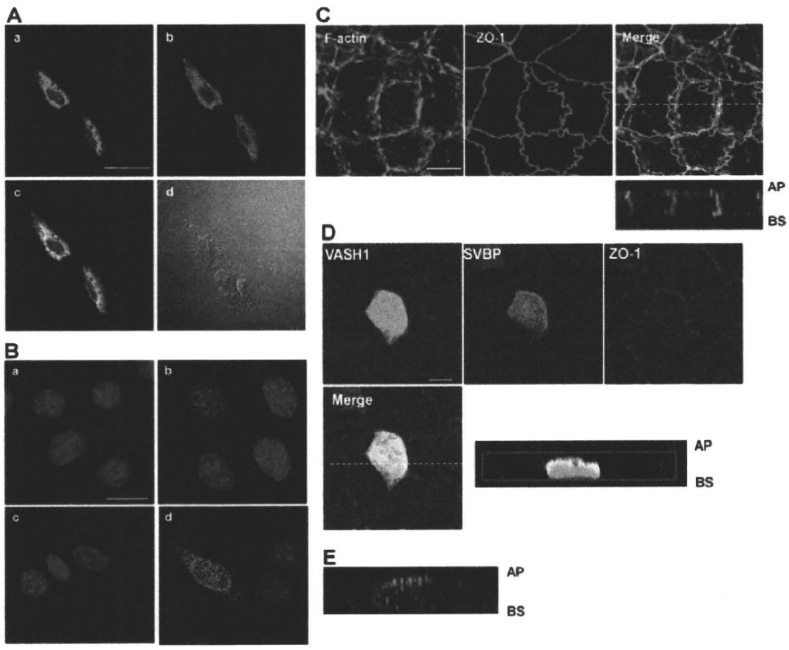

Fig. 4. Intracellular colocalization of SVBP and VASH1. (**A**) Colocalization of SVBP and VASH1 in MS1 cells transiently transfected with a human VASH1 expression vector and p3xFLAG-SVBP for 24 hours. The fixed cells were immunostained with anti-VASH1 (green) and anti-SVBP (red) antibodies. a, VASH1; b, SVBP; c, merge; d, DIC. Scale bar: 50 μm. (**B**) Interaction between SVBP and VASH1 in ECs. PLA was performed after incubation with combination of antibodies. a, normal mouse IgG + normal rabbit IgG; b, normal mouse IgG + anti-Flag antibody; c, anti-VASH1 mAb + normal rabbit IgG; d, anti-VASH1 mAb + anti-Flag antibody. Scale bar: 20 μm. (**C**) MDCK cells with polarization. MDCK cells immunostained with anti-ZO-1 (red, a marker of tight junction) and Phalloidin-FITC (green). Scale bar: 10 μm. (**D**) Apical localization of SVBP in polarized epithelial cells. MDCK cells were transiently co-transfected with human VASH1 and p3xFLAG-SVBP expression vectors for 24 hours. The fixed cells were immunostained with anti-VASH1 (green), anti-FLAG (red) and anti-ZO-1 (blue) antibodies. Scale bar: 10 μm. (**E**) Interaction between SVBP and VASH1 in the apical side of MDCK cells. MDCK cells transiently transfected with human VASH1 and p3xFLAG-SVBP expression vectors were subjected to PLA. AP, apical side; BS, basolateral side.

opposite results (Fig. 5D). SVBP expression did not affect *Vash1* mRNA levels (data not shown), and *Svbp* siRNA specifically decreased endogenous *Svbp* mRNA levels with no effect on the levels of *Vash1* mRNA (Fig. 5E). Also, *Svbp* siRNA decreased the ability to extract VASH1 protein into 1% Triton X-100 cell lysis buffer and decreased the secretion of VASH1 into the medium. These results indicate that SVBP has an important role in VASH1 secretion, probably by increasing the solubility of the VASH1 protein.

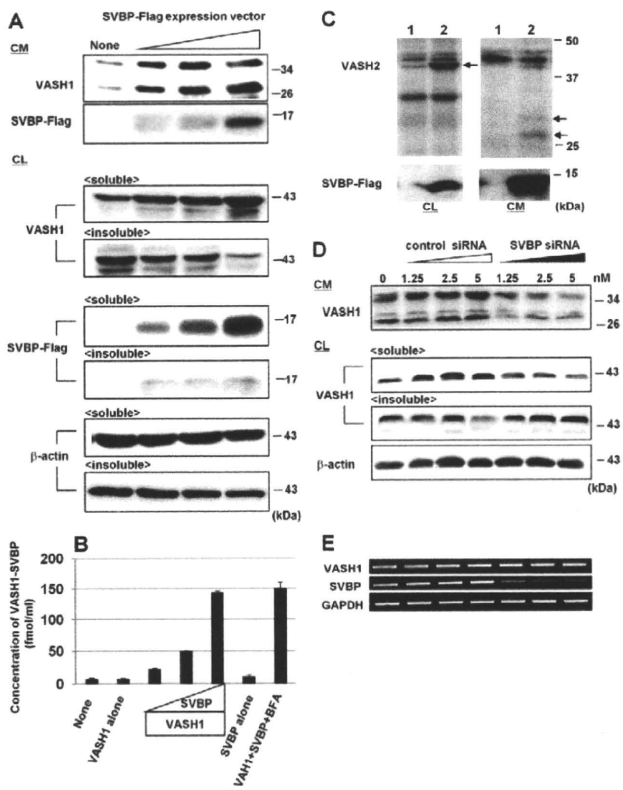

Fig. 5. SVBP increases VASH1 solubility and secretion. (**A**) CM was collected from MS1 cells transiently co-transfected with human VASH1 and various amounts of p3xFLAG-SVBP expression vectors after 24 hours. Concentrated CM, the supernatant (soluble fraction) of cell lysates (CL) and the pellet (insoluble fraction) were evaluated by western blot. (**B**) Measurement of the VASH1–SVBP complex in the CM. The CM was collected from transfected MS1 cells. The concentration of VASH1–SVBP complex in the CM was measured by ELISA. Error bars indicate s.d. BFA, Brefeldin A. (**C**) CL and concentrated CM of MS1 cells transfected with human VASH2 and/or p3xFLAG-SVBP expression vectors were prepared and subjected to western blot analysis. Arrows indicate VASH2 protein in CL or its truncated forms in CM. (**D**) Western blot analysis showed that SVBP knockdown decreases VASH1 secretion and solubility. Concentrated CM and soluble and insoluble fractions of CLs were prepared 48 hours after *VASH1*-expressing MS1 cells were transfected with various concentrations of siRNAs designed against mouse *Svbp* mRNA. (**E**) RT-PCR shows that SVBP knockdown does not affect *Vash1* expression in MS1 cells.

SVBP prevents ubiquitylation of VASH1

The solubility of some proteins in detergent solution is closely concerned with protein folding regulated by interactions with molecular chaperones (Dou et al., 2003; Muchowski et al., 2000). In general, misfolded or unfolded proteins are either refolded by molecular chaperones or degraded immediately by the ubiquitin proteasome system (UPS) (Hishiya and Takayama, 2008; Muchowski et al., 2000), which is known as an intrinsic protein quality control. We hypothesized that SVBP might contribute to the quality control of VASH1 protein in ECs. Therefore, we examined first whether the UPS affects VASH1 stability in ECs. To detect the total amount of VASH1 protein, we prepared cell lysate using 1% SDS cell lysis buffer, which was different to levels in the experiments performed in Fig. 5. As shown in Fig. 6A,B, the

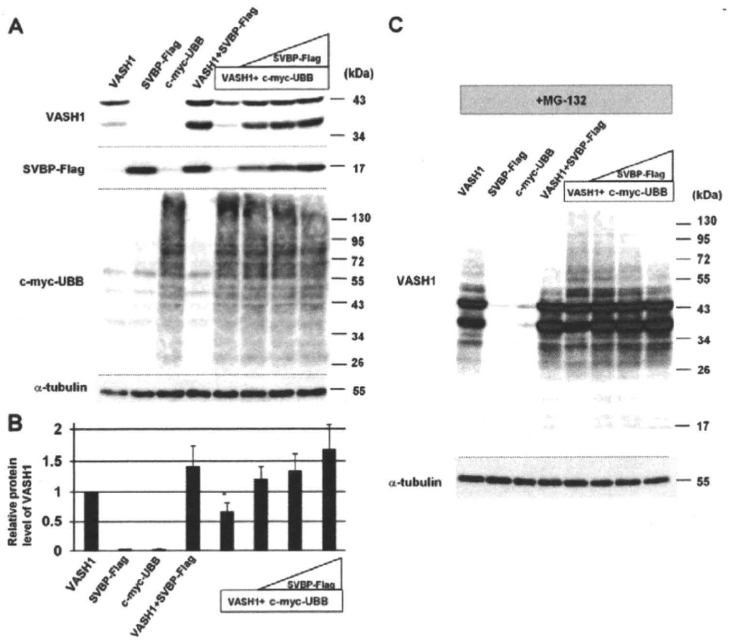

Fig. 6. SVBP inhibits the ubiquitylation of VASH1. (**A**) MS1 cells were transiently transfected with human VASH1, 3xFLAG-SVBP and Myc-UBB expression vectors in the indicated combinations. Cell lysates were prepared and subjected to western blot analysis 24 hours after transfection. (**B**) Densitometric quantification of VASH1 protein. The relative VASH1 protein levels were normalized to α-tubulin. Error bars indicate s.d. (n=3). *P=0.05 versus VASH1 alone. (**C**) Western blot of MS1 cells transiently transfected identically to those in A, but 6 hours after transfection, the cells were incubated with 10 μM MG132 for 18 hours and harvested with cell lysis buffer containing ubiquitin aldehyde.

total amount of VASH1 protein was reduced in the presence of Myc–ubiquitin-B (UBB) compared with VASH1 alone. By contrast, this reduction was recovered in a dose-dependent manner by co-transfection with SVBP, implying that the VASH1 protein is stable when associated with SVBP. In the presence of a proteasome inhibitor, MG-132, polyubiquitylated VASH1 proteins were detected as many ladder bands of a higher molecular mass than the 42 kDa form (Fig. 6C). Co-transfection with SVBP dramatically reduced these polyubiquitylated VASH1 proteins. These results suggest that the interaction between SVBP and VASH1 enhances the stability of VASH1 protein by preventing ubiquitylation.

SVBP accelerates VASH1 function

Finally, we examined whether SVBP affects the anti-angiogenic activity of VASH1. The co-expression of SVBP and VASH1 significantly inhibited VEGF-inducible EC migration (Fig. 7A). Stimulation with VEGF (20 ng/ml) increased MS1 migration 2.2-fold relative to control cells. MS1 cells transfected with VASH1 no longer responded to VEGF stimulation. Co-transfection with VASH1 and SVBP downregulated the basal level of EC migration compared with other samples, regardless of VEGF stimulation. We then examined whether this anti-angiogenic activity might be derived from secreted VASH1. The CM from MDCK cells transfected with VASH1 and/or SVBP expression vector was added to HMVECs. As shown in Fig. 7B, VEGF-inducible migration of HMVECs was inhibited by CM containing the VASH1–SVBP complex in a concentration-dependent manner. These results indicate that SVBP regulates the secretion of VASH from ECs and contributes to the anti-angiogenic activity of VASH1.

Discussion

Secretory proteins generally contain a typical signal sequence composed of successive hydrophobic amino acids that is usually located in the N-terminal region and removed by signal peptidase after the protein passes through the ER membrane (Hegde and Kang, 2008). VASH1 has no such classical secretion signal sequence (Watanabe et al., 2004), and does not colocalize with the ER marker calnexin in ECs (Watanabe et al., 2004). These observations led us to hypothesize that de novo produced VASH1 might be secreted via an unconventional secretory pathway. Here, we identified SVBP as a novel VASH1 binding partner. The association between endogenous SVBP and VASH1 proteins in cell lysate and CM of ECs appeared crucial for VASH1 secretion, because knockdown of SVBP significantly impaired VASH1 secretion. We also showed that SVBP bound to VASH2 and enhanced its secretion from ECs. The expression of *VASH1* mRNA is induced by VEGF or FGF-2, mediated by protein kinase C-δ downstream of VEGF receptor-2 (Shimizu et al., 2005). However, we observed a constitutive expression of *Svbp* mRNA in ECs

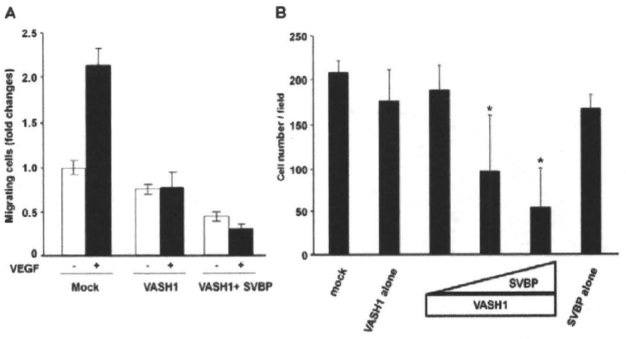

Fig. 7. SVBP accelerates VASH1-mediated inhibition of EC migration. (**A**) MS1 cells were transiently transfected with human VASH1 and/or 3xFLAG-SVBP expression vectors and cell migration analyzed with a modified Boyden chamber assay. Relative numbers of migrating cells are shown as mean ± s.d. (n=3). (**B**) HMVECs were treated with CM collected from MDCK cells transfected human VASH1 and various amounts of p3xFLAG-SVBP expression vectors. Cell migration was analyzed with a modified Boyden chamber assay. The numbers of migrating cells in a field are shown as mean ± s.d. (n=9). *P<0.001 versus negative control (mock).

under basal conditions and in various normal mouse organs. Thus, the scenario of VASH1 secretion might be as follows: SVBP is prepared in advance and accumulates under or on the cell surface. Once VASH1 has been induced, it binds SVBP, which facilitates the secretion of VASH1 (Fig. 8). The molecular mechanism by which VASH1 exhibits anti-angiogenic activity is not fully understood. Co-transfection of VASH1 and SVBP to ECs decreased the basal migration of ECs, suggesting that anti-angiogenic activity of VASH1 might not simply be caused by the blockade of VEGF-mediated signaling in ECs. We predict a putative receptor for VASH1, which transduces specific signals for anti-angiogenesis in ECs. If we could isolate such a receptor, it should help us to characterize the molecular mechanism of VASH activity.

Molecular chaperones comprise several highly conserved families, including heat shock proteins (HSPs), and contribute to post-translational quality control of proteins (Wickner et al., 1999). Although the native structure of a protein is determined principally by its amino acid sequence, the process of folding in vivo often requires the assistance of molecular chaperones, which are often required to maintain the proper conformation of proteins under changing environmental conditions. Misfolded or unfolded proteins exhibit insolubility in detergent solution. Some molecular chaperones can help such proteins to complete the correct folding and recover solubility. For instance, HSP70 and HSP90 are reported to function as molecular chaperones for microtubule-associated protein Tau or endothelial nitric oxide synthase and increase their solubility in detergent solution (Dou et al., 2003; Jiang et al., 2003; Petrucelli et al., 2004). Because SVBP non-covalently binds VASH1 and increases its solubility in 1% Triton X-100 (a nonionic detergent) cell lysis buffer, SVBP might have a chaperone-like role for VASH1. Molecular chaperones, including HSPs, generally accumulate on membranes (Horvath et al., 2008), and our data show that SVBP accumulates on the apical plasma membrane of polarized epithelial cells, supporting a chaperone-like function of SVBP.

Leaderless secretory proteins (e.g. FGF-2, interleukin-1β and galectins) are released from a variety of cell types via unconventional secretory pathways independently of the ER and Golgi (Calderwood et al., 2007; Hughes, 1999; Keller et al., 2008; Nickel, 2005; Nickel and Rabouille, 2009; Piotrowicz et al., 1997; Torrado et al., 2009). Four potential mechanisms of unconventional protein export have been proposed: export across the plasma membrane, export by secretory lysosomes, export through the release of exosomes derived from multivesicular bodies, and export mediated by plasma membrane shedding of microvesicles (Nickel, 2005; Nickel and Rabouille, 2009). Piotrowicz and colleagues previously reported that the molecular chaperone HSP27 binds to FGF-2 in ECs, which facilitates FGF-2 secretion from ECs via an unconventional secretory pathway (Piotrowicz et al., 1997). Importantly, a recent report showed that correctly folded FGF-2 might be required for translocation across the plasma membrane (Torrado et al., 2009). Interestingly, HSPs themselves lack a secretion signal sequence but are released from cells and function as extracellular ligands, giving rise intracellular signaling (Calderwood et al., 2007). However, the detailed mechanism by which molecular chaperones modulate the secretion of leaderless secretory proteins remains obscure. Further study is required to determine whether SVBP is involved in the secretion of other leaderless proteins such as FGF-2.

Recently, the level of *Ccdc23* (also known as SVBP) mRNA was shown to be significantly higher in adenomatous polyposis coli than in normal colorectal mucosa (Gaspar et al., 2008), but the expression of VASH1 appears to be restricted to ECs. Thus, the expression of *Svbp* mRNA might not always associate with the expression of *Vash1* mRNA. SVBP might have additional role(s) beyond that of a VASH1 binding partner. This possibility is currently under investigation.

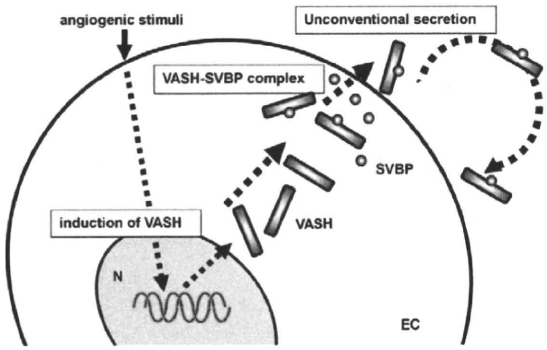

Fig. 8. SVBP facilitates VASH1 secretion by acting as a chaperone. SVBP is constitutively expressed, whereas VASH1 is induced by angiogenic factors (e.g. VEGF and FGF-2) in ECs. SVBP might bind to de novo produced VASH1 and render it soluble via chaperone-like activity, resulting in the efficient secretion of the VASH–SVBP complex into the extracellular space. N, nucleus.

Materials and Methods

Yeast two-hybrid screen

We performed a yeast two-hybrid screen to isolate VASH1 binding partners as previously described (Colland et al., 2004). Full-length human VASH1 (amino acids 1–365) and the human placental random-primed cDNA library were used as bait and prey, respectively. We screened 1.3×10^8 independent clones. The prey fragments of the positive clones were amplified by polymerase chain reaction (PCR) and sequenced. The resulting sequences were used to identify the corresponding gene in the GenBank database.

Plasmid construction

Human *SVBP* cDNA (CCDC23; GenBank accession number NM_199342) was cloned into the *Not*I and *Xba*I sites of the p3xFLAG-CMV14 plasmid vector (Sigma) to generate p3xFLAG-SVBP, in which *SVBP* cDNA was attached to a triple repeat of the FLAG tag sequence at the 3′ end. The DNA fragment containing the *SVBP* cDNA joined with 3xFLAG was cloned into the *Sma*I site of baculovirus transfer vector pYNG (Katakura). Human ubiquitin B cDNA (UBB; GenBank accession number NM_018955) was cloned into the *Eco*RI site of the pCMV Myc plasmid vector (Clontech) to generate pCMV Myc-UBB, in which *UBB* cDNA was attached to a Myc sequence at the 5′ start site.

Evaluation of molecular interactions using the BIAcore system

Recombinant human SVBP-FLAG protein was expressed in the silkworm, *Bombyx mori*, as previously reported (Takahashi et al., 2007). Briefly, the constructed transfer vector was mixed with cysteine-proteinase-deleted baculoviral genomic DNA and then co-transfected in BmN cells of *B. mori* larvae. The resulting recombinant baculovirus was infected in *B. mori* pupae. Harvested pupae were lysed and the SVBP-FLAG protein purified using an anti-FLAG M2 affinity column (Sigma). Purified recombinant full-length VASH1, its truncated forms and VASH2 proteins were prepared as previously described (Shibuya et al., 2006; Sonoda et al., 2006; Watanabe et al., 2004). The interaction of VASH1 and VASH2 with SVBP was analyzed using a BIAcore 3000 (BIAcore AB). SVBP (20.6 μg/ml) in 10 mM sodium acetate (pH 4.5) was immobilized on a CM5 sensor chip using the amine-coupling method according to the manufacturer's protocol. VASH1, its truncated forms, or VASH2 in 10 mM HEPES (pH 7.4), 0.15 M NaCl, 3 mM EDTA, 0.005% Surfactant P20 (pH 7.4) at concentrations of 62.5 nM to 1 μM was passed over the surface of the sensor chip at a flow rate of 20 μl/minute. The interaction was monitored as the change in surface plasmon resonance response at 25°C. After 2 minutes of monitoring, the same buffer was introduced to the sensor chip in place of the VASH1 solution to start the dissociation. The sensor surface was regenerated with 10 mM glycine (pH 2.0) at the end of each experiment. Both the association rate constant (K_a) and the dissociation rate constant (K_d) were calculated according to the BIAevaluation software. The dissociation constant (K_D) was determined as K_d/K_a.

Cell culture

The murine EC line MS1 was cultured in α minimal essential medium (αMEM; Wako Pure Chemical) supplemented with 10% fetal bovine serum (FBS; JRH Biosciences) (Arbiser et al., 1997). Polarized epithelial Madin-Darby canine kidney (MDCK) cells were cultured in Dulbecco's modified Eagle medium (Wako Pure Chemical) supplemented with 10% FBS (Martin-Belmonte et al., 2001). Human umbilical vein endothelial cells (HUVECs) and human microvascular endothelial cells (HMVECs) were purchased from KURABO and cultured on type I-C collagen-coated dishes (Asahi Techno Glass) in endothelial basal medium containing 5% FBS and EC growth supplements (Cambrex Bio Science Walkersville).

RT-PCR

Total RNA was extracted from cultured cells using the RNeasy Mini Kit (Qiagen). RT-PCR was carried out using the First Strand cDNA Synthesis Kit (Roche Diagnostics) according to the manufacturer's instructions. Briefly, total RNA was reverse transcribed for 50 minutes at 42°C using oligo(dT) primers. PCR was performed using sets of primers specific for the target genes. Thermal cycler conditions were 20–30 cycles of 94°C for 15 seconds for denaturing, 56°C for 30 seconds for annealing and 72°C for 45 seconds for extension. PCR products were separated on a 1.5% agarose gel and visualized under ultraviolet by ethidium bromide staining. The primer pairs were as follows: mouse *Ccdc23*, sense (5′-ATGGATCCACCTGCCCGGAA-3′) and antisense (5′-TCACTCCCCAGGCGGCTGCA-3′); mouse *Vash1*, sense (5′-ATGTGGAAGGCATGTGGCCAAG-3′) and antisense (5′-CACCCGGATCTGGTACCCACT-3′).

Northern blotting

Total RNA was isolated from cultured cells or mouse organs using QIAzol reagent (Qiagen), and mRNA was isolated from total RNA samples using Oligotex-dT30 Super (Takara) according to the manufacturers' instructions. Each mRNA sample (600 ng) was separated by 1% agarose-formaldehyde gel electrophoresis and transferred to a positively charged nylon membrane (Roche Diagnostics). Membranes were hybridized with antisense SVBP- or β-actin-specific RNA probes labeled with digoxigenin (DIG) using the SP6/T7 DIG RNA Labeling Kit (Roche Diagnostics). Hybridization was performed for 2 hours at 68°C using PerfectHyb reagent (Toyobo) containing 0.2 ng/ml DIG-labeled antisense RNA probe, After hybridization, the membranes were washed twice with 2× SSC, 0.1% sodium dodecyl sulfate (SDS) at 68°C for 15 minutes. The final wash was performed twice using 0.1× SSC, 0.1% SDS at 68°C for 15 minutes. The mRNA bands were detected using the Northern Blot Starter Kit (Roche Diagnostics), and the results were analyzed using a LAS-4000 (Fuji Photo Film).

Small interfering RNAs (siRNAs)

Three sets of specific siRNAs targeting mouse *Svbp* mRNA (mouse CCDC23; GenBank accession number NM_024462) were designed and synthesized by Invitrogen. The target sequences were: *Svbp* siRNA A, 5′-GGGUCAGAGCUAACCAAGAAGCAUU-3′; *Svbp* siRNA B, 5′-AAGAAGCAUUCAGAAGCCAAACCAU-3′; *Svbp* siRNA C, 5′-GAGAUCUAUGCUCUCAACAGAGUCA-3′. Stealth RNAi Negative Control Low GC Duplex (Invitrogen) was used as a negative control. Cells were cultured to 60–70% confluency and transfected with *Svbp* siRNAs using Lipofectamine RNAiMAX (Invitrogen) according to the manufacturer's instructions. The medium was changed after 3 hours of transfection and the cells cultured for an additional 24–48 hours.

Transient transfection

MS1 and MDCK cells were transiently transfected with human VASH1 (Watanabe et al., 2004), human VASH2 (Shibuya et al., 2006), p3xFLAG-SVBP, and pCMV Myc-UBB expression vectors using Effectene reagent (Qiagen) according to the manufacturer's instructions.

Preparation of anti-SVBP monoclonal antibodies

A/J mice (Japan SLC) were immunized three times with Cys-SVBP peptide (Asp2–Lys13 of the CCDC23 protein) conjugated to keyhole limpet hemocyanin. Spleen cells from the immunized mice were fused with the myeloma cell line P3U1. Culture supernatant from each hybridoma was screened as previously described (Ohta et al., 1999; Watanabe et al., 2004). Positive hybridomas were cloned using the limiting-dilution technique. The resulting monoclonal antibodies (mAbs) were purified from ascites using protein-A–Sepharose beads (GE Healthcare Bio-Sciences).

Western blotting

Cells were lysed in 1% SDS cell lysis buffer consisting of 10 mM Tris-HCl, pH 7.5, 150 mM NaCl, 1% SDS supplemented with 0.5 mM phenylmethylsulfonyl fluoride and Complete EDTA-free Protease Inhibitor Cocktail (Roche Diagnostics). The CM was concentrated 50-fold using an Amicon Ultra-15 (10,000 MWCO; Millipore). Equal amounts of protein from cell lysates and concentrated CM were separated by SDS-polyacrylamide gel electrophoresis (SDS-PAGE) and transferred onto polyvinylidene fluoride (PVDF) membranes (Bio-Rad). Blotting was performed according to standard procedures. The primary antibodies were anti-human VASH1 mAb (Watanabe et al., 2004), anti-human VASH2 mAb (Shibuya et al., 2006), anti-human SVBP mAb, anti-FLAG M2 mAb (Sigma), and anti-Myc mAb (Clontech). Normalization was performed using anti-β-actin mAb (Sigma). Immunoreactive protein bands were detected using ECL Western Blotting Detection Reagents (GE Healthcare) or Immobilon Western HRP Substrate (Millipore) using an LAS-4000 (Fuji Photo Film). Densitometric quantification was performed using Multi Gauge Ver 3.0 software (Fuji Photo Film).

Extraction of soluble and insoluble VASH1 proteins from cultured cells

Cells were lysed in ice-cold 1% Triton X-100 cell lysis buffer consisting of 10 mM Tris-HCl, pH 7.5, 150 mM NaCl, 1% sodium deoxycholate, 0.1% SDS, and 1% Triton X-100. Cell extracts were placed on ice for 1 hour and then centrifuged at 15,000 ***g*** for 15 minutes to separate the supernatant (soluble fraction) and pellet (insoluble fraction). The insoluble fraction was washed three times with ice-cold 1% Triton X-100 cell lysis buffer and re-extracted with sample buffer for SDS-PAGE. Western blotting was carried out as described above.

Immunoprecipitation

The cell lysate or CM was incubated with anti-human VASH1 antibody, anti-human SVBP antibody, or normal mouse IgG (Santa Cruz Biotechnology) at 4°C overnight on a rotating mixer. Protein-A–Sepharose beads were then added and the samples incubated for another 2 hours at 4°C. The beads were washed three times with phosphate-buffered saline (PBS) containing 0.05% Tween 20. Immunoprecipitated proteins were eluted into sample buffer for SDS-PAGE, and western blotting was performed as described above.

Immunostaining

Transfected MS1 or MDCK cells were fixed in 4% paraformaldehyde, permeabilized with 0.1% Triton-X100, and stained with VASH1, SVBP, FLAG (Sigma), ZO-1 (Sanko Junyaku) antibodies, or Phalloidin-FITC (Sigma). Nuclei were visualized using TO-PRO®3 (Invitrogen). All incubations were performed at 4°C in PBS containing 1% bovine serum albumin. Images were captured using a Fluoview FV1000 confocal microscope system (Olympus).

Duolink in situ proximity ligation assay (PLA)

The Duolink in situ PLA kit was purchased from Olink Bioscience. Transfected MS1 cells and MDCK cells were immunoreacted with the combination of anti-human VASH1 mAb (mouse), anti-FLAG plyclonal Ab (rabbit), normal mouse IgG, and normal rabbit IgG as described above. According to the manufacturer's protocol, a pair of anti-mouse MINUS and anti-rabbit PLUS was used to generate positive fluorescence signals indicating that two PLA probes bound in close proximity (<40 nm). Nuclei counterstaining using TO-PRO®3 and the images were captured as described above.

ELISA for VASH1-SVBP complex

We established a highly sensitive ELISA system that could quantify the VASH1–SVBP complex. A pair of specific monoclonal antibody against SVBP and VASH1 was used to coat a 96-well plate and for HRP labeling, respectively. MS1 cells and MDCK cells were transiently co-transfected with a combination of human VASH1 and SVBP expression vectors for 6 hours, then were washed with serum free α-MEM, and cultured in 0.1% FBS in α-MEM for 24 hours. The CMs were centrifuged at 5000 ***g*** for 15 minutes to remove cell debris. Subsequently, the supernatant was subjected to ELISA. The detailed procedure for the measurements carried out is described elsewhere (Heishi et al., 2010).

Endothelial cell migration

The migratory activity of ECs was measured by modified Boyden chamber assay in two different procedures (Kobayashi et al., 2006; Watanabe et al., 2004). First, transfected MS1 cells were plated on the upper chambers (inserts) of the Boyden chamber (8.0 μm pore size, Corning). The lower chamber was filled with 0.2% FBS in α-MEM with or without 20 ng/ml recombinant human VEGF (Sigma). After incubation for 18 hours, cells that migrated to the lower surface of the membrane were fixed with 4% formaldehyde, stained with crystal violet (Sigma), and counted in a blinded manner. The relative number of migrating cells was calculated; the mean number of migrating cells transfected with empty vector (mock) alone was set equal to 1.0.

Another procedure was prepared to evaluate anti-angiogenic activity of the VASH1–SVBP complex secreted from cells. MDCK cells were transiently co-transfected with a combination of human VASH1 and SVBP expression vectors for 6 hours, washed with serum free α-MEM and then cultured in 0.05% FBS in α-MEM for 24 hours. CM was concentrated 10-fold using an Amicon Ultra-15. HMVECs, preincubated in 0.5% FBS in Medium-199 (Invitrogen) for 16 hours, were suspended in concentrated CMs and then plated on the upper chambers of the Boyden chamber. The lower chamber was filled with 0.5% FBS in Medium-199 with 20 ng/ml recombinant human VEGF. HMVECs were allowed to migrate under VEGF stimulation for 4 hours. The number of cells that migrated across the filter was counted in nine fields per insert in a blinded manner.

Statistical analysis

Data are expressed as mean ± s.d. Significance was assessed by one-way analysis of variance (ANOVA) followed by Sheffe's *t*-test.

This study was supported by the Grant-in-Aid for Scientific Research on Priority Areas (17014006) and the Grant-in-Aid for Young Scientists (19790509) from the Ministry of Education, Culture, Sports, Science, and Technology of Japan.

References

Arbiser, J. L., Moses, M. A., Fernandez, C. A., Ghiso, N., Cao, Y., Klauber, N., Frank, D., Brownlee, M., Flynn, E., Parangi, S. et al. (1997). Oncogenic H-ras stimulates tumor angiogenesis by two distinct pathways. *Proc. Natl. Acad. Sci. USA* **94**, 861-866.

Calderwood, S. K., Mambula, S. S. and Gray, P. J., Jr (2007). Extracellular heat shock proteins in cell signaling and immunity. *Ann. NY Acad. Sci.* **1113**, 28-39.

Carmeliet, P. (2003). Angiogenesis in health and disease. *Nat. Med.* **9**, 653-660.

Colland, F., Jacq, X., Trouplin, V., Mougin, C., Groizeleau, C., Hamburger, A., Meil, A., Wojcik, J., Legrain, P. and Gauthier, J. M. (2004). Functional proteomics mapping of a human signaling pathway. *Genome Res.* **14**, 1324-1332.

Dou, F., Netzer, W. J., Tanemura, K., Li, F., Hartl, F. U., Takashima, A., Gouras, G. K., Greengard, P. and Xu, H. (2003). Chaperones increase association of tau protein with microtubules. *Proc. Natl. Acad. Sci. USA* **100**, 721-726.

Gaspar, C., Cardoso, J., Franken, P., Molenaar, L., Morreau, H., Moslein, G., Sampson, J., Boer, J. M., de Menezes, R. X. and Fodde, R. (2008). Cross-species comparison of human and mouse intestinal polyps reveals conserved mechanisms in adenomatous polyposis coli (APC)-driven tumorigenesis. *Am. J. Pathol.* **172**, 1363-1380.

Hegde, R. S. and Kang, S. W. (2008). The concept of translocational regulation. *J. Cell Biol.* **182**, 225-232.

Heishi, T., Hosaka, T., Suzuki, Y., Miyashita, H., Oike, Y., Takahashi, T., Nakamura, T., Arioka, S., Mitsuda, Y., Takakura, T. et al. (2010). Endogenous angiogenesis inhibitor vasohibin1 exhibits broad-spectrum antilymphangiogenic activity and suppresses lymph node metastasis. *Am. J. Pathol.* **176**, 1950-1958.

Hellstrom, M., Phng, L. K., Hofmann, J. J., Wallgard, E., Coultas, L., Lindblom, P., Alva, J., Nilsson, A. K., Karlsson, L., Gaiano, N. et al. (2007). Dll4 signalling through Notch1 regulates formation of tip cells during angiogenesis. *Nature* **445**, 776-780.

Hishiya, A. and Takayama, S. (2008). Molecular chaperones as regulators of cell death. *Oncogene* **27**, 6489-6506.

Horvath, I., Multhoff, G., Sonnleitner, A. and Vigh, L. (2008). Membrane-associated stress proteins: more than simply chaperones. *Biochim. Biophys. Acta* **1778**, 1653-1664.

Hosaka, T., Kimura, H., Heishi, T., Suzuki, Y., Miyashita, H., Ohta, H., Sonoda, H., Moriya, T., Suzuki, S., Kondo, T. et al. (2009). Vasohibin-1 expression in endothelium of tumor blood vessels regulates angiogenesis. *Am. J. Pathol.* **175**, 430-439.

Hughes, R. C. (1999). Secretion of the galectin family of mammalian carbohydrate-binding proteins. *Biochim. Biophys. Acta* **1473**, 172-185.

Jiang, J., Cyr, D., Babbitt, R. W., Sessa, W. C. and Patterson, C. (2003). Chaperone-dependent regulation of endothelial nitric-oxide synthase intracellular trafficking by the co-chaperone/ubiquitin ligase CHIP. *J. Biol. Chem.* **278**, 49332-49341.

Keller, M., Ruegg, A., Werner, S. and Beer, H. D. (2008). Active caspase-1 is a regulator of unconventional protein secretion. *Cell* **132**, 818-831.

Kerbel, R. S. (2008). Tumor angiogenesis. *N. Engl. J. Med.* **358**, 2039-2049.

Kimura, H., Miyashita, H., Suzuki, Y., Kobayashi, M., Watanabe, K., Sonoda, H., Ohta, H., Fujiwara, T., Shimosegawa, T. and Sato, Y. (2009). Distinctive localization and opposed roles of vasohibin-1 and vasohibin-2 in the regulation of angiogenesis. *Blood* **113**, 4810-4818.

Kobayashi, M., Nishita, M., Mishima, T., Ohashi, K. and Mizuno, K. (2006). MAPKAPK-2-mediated LIM-kinase activation is critical for VEGF-induced actin remodeling and cell migration. *EMBO J.* **25**, 713-726.

Leslie, J. D., Ariza-McNaughton, L., Bermange, A. L., McAdow, R., Johnson, S. L. and Lewis, J. (2007). Endothelial signalling by the Notch ligand Delta-like 4 restricts angiogenesis. *Development* **134**, 839-844.

Martin-Belmonte, F., Arvan, P. and Alonso, M. A. (2001). MAL mediates apical transport of secretory proteins in polarized epithelial Madin-Darby canine kidney cells. *J. Biol. Chem.* **276**, 49337-49342.

Muchowski, P. J., Schaffar, G., Sittler, A., Wanker, E. E., Hayer-Hartl, M. K. and Hartl, F. U. (2000). Hsp70 and hsp40 chaperones can inhibit self-assembly of polyglutamine proteins into amyloid-like fibrils. *Proc. Natl. Acad. Sci. USA* **97**, 7841-7846.

Nasu, T., Maeshima, Y., Kinomura, M., Hirokoshi-Kawahara, K., Tanabe, K., Sugiyama, H., Sonoda, H., Sato, Y. and Makino, H. (2009). Vasohibin-1, a negative feedback regulator of angiogenesis, ameliorates renal alterations in a mouse model of diabetic nephropathy. *Diabetes* **58**, 2365-2375.

Nickel, W. (2005). Unconventional secretory routes: direct protein export across the plasma membrane of mammalian cells. *Traffic* **6**, 607-614.

Nickel, W. (2007). Unconventional secretion: an extracellular trap for export of fibroblast growth factor 2. *J. Cell Sci.* **120**, 2295-2299.

Nickel, W. and Rabouille, C. (2009). Mechanisms of regulated unconventional protein secretion. *Nat. Rev. Mol. Cell Biol.* **10**, 148-155.

Ohta, H., Tsuji, T., Asai, S., Sasakura, K., Teraoka, H., Kitamura, K. and Kangawa, K. (1999). One-step direct assay for mature-type adrenomedullin with monoclonal antibodies. *Clin. Chem.* **45**, 244-251.

Petrucelli, L., Dickson, D., Kehoe, K., Taylor, J., Snyder, H., Grover, A., De Lucia, M., McGowan, E., Lewis, J., Prihar, G. et al. (2004). CHIP and Hsp70 regulate tau ubiquitination, degradation and aggregation. *Hum. Mol. Genet.* **13**, 703-714.

Piotrowicz, R. S., Martin, J. L., Dillman, W. H. and Levin, E. G. (1997). The 27-kDa heat shock protein facilitates basic fibroblast growth factor release from endothelial cells. *J. Biol. Chem.* **272**, 7042-7047.

Sabath, E., Negoro, H., Beaudry, S., Paniagua, M., Angelow, S., Shah, J., Grammatikakis, N., Yu, A. S. and Denker, B. M. (2008). Galpha12 regulates protein interactions within the MDCK cell tight junction and inhibits tight-junction assembly. *J. Cell Sci.* **121**, 814-824.

Sato, H., Abe, T., Wakusawa, R., Asai, N., Kunikata, H., Ohta, H., Sonoda, H., Sato, Y. and Nishida, K. (2009). Vitreous levels of vasohibin-1 and vascular endothelial growth factor in patients with proliferative diabetic retinopathy. *Diabetologia* **52**, 359-361.

Sato, Y. (2006). Update on endogenous inhibitors of angiogenesis. *Endothelium* **13**, 147-155.

Sato, Y. and Sonoda, H. (2007). The vasohibin family: a negative regulatory system of angiogenesis genetically programmed in endothelial cells. *Arterioscler. Thromb. Vasc. Biol.* **27**, 37-41.

Seelenmeyer, C., Wegehingel, S., Lechner, J. and Nickel, W. (2003). The cancer antigen CA125 represents a novel counter receptor for galectin-1. *J. Cell Sci.* **116**, 1305-1318.

Shen, J., Yang, X., Xiao, W. H., Hackett, S. F., Sato, Y. and Campochiaro, P. A. (2006). Vasohibin is up-regulated by VEGF in the retina and suppresses VEGF receptor 2 and retinal neovascularization. *FASEB J.* **20**, 723-725.

Shibuya, T., Watanabe, K., Yamashita, H., Shimizu, K., Miyashita, H., Abe, M., Moriya, T., Ohta, H., Sonoda, H., Shimosegawa, T. et al. (2006). Isolation and characterization of vasohibin-2 as a homologue of VEGF-inducible endothelium-derived angiogenesis inhibitor vasohibin. *Arterioscler. Thromb. Vasc. Biol.* **26**, 1051-1057.

Shimizu, K., Watanabe, K., Yamashita, H., Abe, M., Yoshimatsu, H., Ohta, H., Sonoda, H. and Sato, Y. (2005). Gene regulation of a novel angiogenesis inhibitor, vasohibin, in endothelial cells. *Biochem. Biophys. Res. Commun.* **327**, 700-706.

Siekmann, A. F. and Lawson, N. D. (2007). Notch signalling limits angiogenic cell behaviour in developing zebrafish arteries. *Nature* **445**, 781-784.

Sonoda, H., Ohta, H., Watanabe, K., Yamashita, H., Kimura, H. and Sato, Y. (2006). Multiple processing forms and their biological activities of a novel angiogenesis inhibitor vasohibin. *Biochem. Biophys. Res. Commun.* **342**, 640-646.

Takahashi, T., Tada, M., Igarashi, S., Koyama, A., Date, H., Yokoseki, A., Shiga, A., Yoshida, Y., Tsuji, S., Nishizawa, M. et al. (2007). Aprataxin, causative gene product for EAOH/AOA1, repairs DNA single-strand breaks with damaged 3′-phosphate and 3′-phosphoglycolate ends. *Nucleic Acids Res.* **35**, 3797-3809.

Tamaki, K., Moriya, T., Sato, Y., Ishida, T., Maruo, Y., Yoshinaga, K., Ohuchi, N. and Sasano, H. (2009). Vasohibin-1 in human breast carcinoma: a potential negative feedback regulator of angiogenesis. *Cancer Sci.* **100**, 88-94.

Torrado, L. C., Temmerman, K., Muller, H. M., Mayer, M. P., Seelenmeyer, C., Backhaus, R. and Nickel, W. (2009). An intrinsic quality-control mechanism ensures unconventional secretion of fibroblast growth factor 2 in a folded conformation. *J. Cell Sci.* **122**, 3322-3329.

Wakusawa, R., Abe, T., Sato, H., Yoshida, M., Kunikata, H., Sato, Y. and Nishida, K. (2008). Expression of vasohibin, an antiangiogenic factor, in human choroidal neovascular membranes. *Am. J. Ophthalmol.* **146**, 235-243.

Watanabe, K., Hasegawa, Y., Yamashita, H., Shimizu, K., Ding, Y., Abe, M., Ohta, H., Imagawa, K., Hojo, K., Maki, H. et al. (2004). Vasohibin as an endothelium-derived negative feedback regulator of angiogenesis. *J. Clin. Invest.* **114**, 898-907.

Wickner, S., Maurizi, M. R. and Gottesman, S. (1999). Posttranslational quality control: folding, refolding, and degrading proteins. *Science* **286**, 1888-1893.

Yamashita, H., Abe, M., Watanabe, K., Shimizu, K., Moriya, T., Sato, A., Satomi, S., Ohta, H., Sonoda, H. and Sato, Y. (2006). Vasohibin prevents arterial neointimal formation through angiogenesis inhibition. *Biochem. Biophys. Res. Commun.* **345**, 919-925.

Yamazaki, T., Yoshimatsu, Y., Morishita, Y., Miyazono, K. and Watabe, T. (2009). COUP-TFII regulates the functions of Prox1 in lymphatic endothelial cells through direct interaction. *Genes Cells* **14**, 425-434.

Yoshinaga, K., Ito, K., Moriya, T., Nagase, S., Takano, T., Niikura, H., Yaegashi, N. and Sato, Y. (2008). Expression of vasohibin as a novel endothelium-derived angiogenesis inhibitor in endometrial cancer. *Cancer Sci.* **99**, 914-919.

Cancer Science
The official journal of the Japanese Cancer Association

Roles of intrinsic angiogenesis inhibitor, vasohibin, in cervical carcinomas

Kousuke Yoshinaga,[1,5] Kiyoshi Ito,[1] Takuya Moriya,[2] Satoru Nagase,[1] Tadao Takano,[1] Hitoshi Niikura,[1] Hironobu Sasano,[3] Nobuo Yaegashi[1] and Yasufumi Sato[4]

[1]Department of Gynecology, Tohoku University Graduate School of Medicine, Sendai; [2]Department of Pathology, Kawasaki Medical School, Kawasaki; [3]Department of Pathology, Tohoku University Graduate School of Medicine, Sendai; [4]Department of Vascular Biology, Institute of Development, Aging, and Cancer, Tohoku University, Sendai, Japan

(Received September 24, 2010/Revised November 11, 2010/Accepted November 18, 2010/Accepted manuscript online November 26, 2010/Article first published online December 22, 2010)

The aim of the present study is to clarify the critical roles of vasohibin in cervical carcinomas. We investigated the expression ratios of vasohibin and vascular endothelial growth factor (VEGF) receptor-2 on endothelium and microvessel density, lymphatic vessel density (LVD) by immunohistochemistry. Sixty-one squamous cell carcinoma (SCC), 18 mucinous adenocarcinoma (Adenocarcinoma), 38 carcinoma *in situ* (CIS), and 35 normal cervical epithelium were collected. We investigated the expression of vasohibin and compared it with the expression of VEGF receptor-2 (VEGFR-2, KDR/flk-1), and CD34 in the stromal endothelium. Expression of VEGF was counted using the histological score (H score). D2-40 was used as a marker for lymphatic endothelial cells to investigate LVD. The microvessel density of the normal cervical epithelium was significantly lower than that of CIS, SCC, and Adenocarcinoma ($P < 0.05$). The expression ratio of vasohibin in the normal cervical epithelium was significantly lower than that of SCC and Adenocarcinoma ($P < 0.05$). The expression ratio of VEGFR-2 of the normal cervical epithelium was significantly lower than that of SCC and Adenocarcinoma ($P < 0.05$). The LVD of the normal cervical epithelium was significantly lower than that of CIS, SCC, and Adenocarcinoma ($P < 0.05$). For normal cervical epithelium, CIS, and SCC, there was a moderate correlation between the expression percentage of vasohibin and the expression percentage of VEGFR-2 ($P < 0.05$, $r^2 = 0.3018$). This is the first study to elucidate the correlation between the expression of vasohibin in the stromal endothelial cells and the expression of VEGFR-2 in human cervical carcinomas. (*Cancer Sci* 2011; 102: 446–451)

Cervical carcinoma is a common gynecologic malignancy in women worldwide. In 2008 in the USA, an estimated 11 070 new cases of invasive cervical cancer were diagnosed and 3870 cancer-related deaths were expected to occur; this represents approximately 1% of cancer deaths in women.[1] The morbidity of cervical cancer, especially in women younger than 40 years old, is rapidly increasing and is the worst in Japan.[2] It is well recognized that angiogenesis (the process of forming new vessels) is required for tumor growth and enables the hematogenous spread of tumor cells throughout the cervical cancer. Several studies document the association between the MVD and/or the extent of endothelial proliferation, the pre-cancer and tumor stage, and the invasive disease of the cervical cancer.[3–6] The expression of various angiogenesis stimulators, such as VEGFs, angiopoietins, and thymidine phosphorylase, has been reported in cervical cancer and dysplasia.[7,8] Several published reports similarly report stromal LVD in cervical neoplasia.[9–11] Angiogenesis is determined by the local balance between angiogenic stimulators and inhibitors. However, the significance of endogenous angiogenesis inhibitors in cervical cancer is poorly documented.

We isolated a novel angiogenesis inhibitor, vasohibin, which is specifically expressed in ECs. Its basal expression in quiescent ECs is low; however, its production is induced by angiogenic stimuli such as VEGF-A and fibroblast growth factor-2, and it inhibits angiogenesis in an autocrine manner.[12,13] We therefore propose that vasohibin acts as a negative feedback regulator to inhibit angiogenesis. VEGF-A is the most important factor for angiogenesis and most VEGF-A-mediated signals for angiogenesis are transduced through VEGF receptor-2 (VEGFR-2).[14] We observed that the VEGF-A-mediated induction of vasohibin was preferentially mediated through the VEGFR-2 signaling pathway.[15] In human cancer tissues, we have already reported a significant correlation between the expression ratio of vasohibin and VEGFR-2 in the vascular endothelial cells of endometrial cancer and breast cancer.[16–18]

In the present study, we aimed to elucidate the significance of vasohibin in human cervical cancer and in the normal cervical squamous epithelium. We investigated the correlations between a tumor's biology (including vasohibin) and the clinical prognostic factors for cervical cancer (such as MVD, LVD, and the expression rate of vasohibin and VEGFR-2 in the endothelial cells). The histological type, lymph node metastasis, vessel involvement, and staging were the most important prognostic factors for cervical cancer. Our analysis revealed a significantly positive correlation between vasohibin and VEGFR-2 in cervical cancer. This is the first study to profile the expression of vasohibin as a negative feedback regulator of angiogenesis in human cervical cancer.

Materials and Methods

Tissue specimens and clinical data. There were 61 SCC, 18 mucinous adenocarcinoma (Adenocarcinoma), 38 CIS, and 35 normal cervical epithelium. Of the 61 SCC: 11 were stage IA (lymph node metastasis 0/11, vessel involvement 0/11, parametrium invasion 0/11); 29 were stage IB (lymph node metastasis 6/29, vessel involvement 11/29, parametrium invasion 0/29); 12 were stage IIA (lymph node metastasis 3/12, vessel involvement 7/12, parametrium invasion 0/12); and nine were stage IIB (lymph node metastasis 4/9, vessel involvement 6/9, parametrium invasion 8/9). Of the 18 mucinous adenocarcinomas: three were stage IA (lymph node metastasis 0/3, vessel involvement 1/3, parametrium invasion 0/3); 11 were stage IB (lymph node metastasis 1/11, vessel involvement 0/11, parametrium invasion 0/11); and four were stage IIB (lymph node metastasis 3/4, vessel involvement 4/4, parametrium invasion 3/4). We investigated the expression of vasohibin, and compared it with the expression of VEGFR-2 (KDR/flk-1)and CD34 (as a marker for vascular endothelial cells) in the stromal vascular endothelium. We used VEGF to indicate the presence of carcinoma cells and normal squamous epithelium. To investigate MVD, CD34

[5]To whom correspondence should be addressed.
E-mail: y-kou-m@mtb.biglobe.ne.jp

doi: 10.1111/j.1349-7006.2010.01812.x

was used as a marker for vascular endothelial cells. To investigate LVD, D2-40 was used as a marker for lymphatic endothelial cells. Immunohistochemical assessment was classified as negative or positive, based on the staining intensity.

Tissue specimens were retrieved from the surgical pathology files of Tohoku University Hospital (Sendai, Japan). The Ethics Committee at Tohoku University School of Medicine (Sendai, Japan) approved the protocol for this study.

The average age was 43.1 years in patients with SCC, 47.1 years old in patients with adenocarcinomas; and 41.0 years old in patients with CIS. Each patient provided written, informed consent before her surgery. None of the patients who were examined had received irradiation, hormonal therapy, or chemotherapy prior to surgery. The clinicopathological findings of the patients (including age, histology, stage, grade, and preoperative therapy) were retrieved by an extensive review of the charts. The standard primary treatment for cervical carcinoma at the Tohoku University Hospital was surgery, which consisted of abdominal radical hysterectomy and pelvic lymphadenectomy. The lesions were classified according to the Histological Typing of Female Genital Tract Tumors by the World Health Organization and staged in accordance with the International Federation of Gynecology and Obstetrics system.[19,20] Patients with subtypes other than CIS, SCC, or mucinous adenocarcinoma, or patients who had second primary carcinoma, were excluded from this series.

All specimens were routinely processed (i.e., 10% formalin and fixed for 24–48 h), embedded in paraffin, and thin sectioned (3 μm).

Immunohistochemical staining and the scoring of immunoreactivity. We carried out immunohistochemical staining for vasohibin, VEGFR-2, CD34 (as a marker for vascular endothelial cells), and D2-40 (as a lymphatic vessel marker). The presence of VEGF-A was assessed in normal squamous epithelium and in carcinoma cells. Paraffin-embedded tissue sections from human endometrial cancers were deparaffinized, rehydrated, and incubated with 3% H_2O_2 for 10 min to block endogenous peroxidase activity. The sections were incubated for 30 min at room temperature in a blocking solution of 10% goat serum (Nichirei Biosciences, Tokyo, Japan). They were then stained for 12 h at 4°C with primary antibodies, followed by staining for 30 min at room temperature with secondary antibodies. The primary antibodies were all mouse mAbs and were used as follows: 2 μg/mL anti-human vasohibin mAb, anti-VEGFR-2 (Santa Cruz Biotechnology, Santa Cruz, CA, USA) diluted at 1:100; anti-CD34 (Dako, Copenhagen, Denmark) diluted at 1:200; anti-D2-40 (Dako) diluted at 1:100; and anti-VEGF-A (Lab Vision, Fremont, CA, USA) diluted at 1:100. We previously described a mouse mAb against a synthetic peptide corresponding to the 286–299 amino acid sequence of vasohibin.[15] The positive control slide for CD34 antigen was prepared from paraffin-fixed breast cancer tissue that contained a high microvessel density. Nuclei were counterstained with hematoxylin.

Three investigators (K.A., T.E., and K.Y) independently evaluated the immunohistochemical staining of the entire group of tissue sections. They were blinded to the clinical course of the patients. The average number counted by the three investigators was used for subsequent analysis.

We carefully examined the areas where cancer cells had come in contact with or had invaded the stroma. After first scanning the immunostained section at low magnification, microvessels having CD34-positive signals were counted. The areas with the greatest number of distinctly highlighted microvessels were selected. Any cell clusters with CD34-positive signals were regarded as a single countable microvessel, regardless of whether the lumen was visible. Unstained lumina were considered artifacts, even if they contained blood or tumor cells. Microvessel density was assessed by light microscopy in areas of invasive tumor containing the highest number of capillaries and small venules per area (i.e., neovascular hot spots), in accordance with an original method.[21] Lymphatic vessel density was investigated by D2-40-positive signals, using the same procedure described as above.

Immunostaining for vasohibin and VEGFR-2 was evaluated in the serial thin sections. Positive immunoreactive signals for vasohibin and VEGFR-2 in CD34-positive microvessels were counted; from this the positive ratios of vasohibin and VEGFR-2 in microvessels were calculated. Using an established antibody, immunohistochemistry detected the protein expression of a selected angiogenic factor (i.e., VEGF-A). For this marker, the intensity of cytoplasmic staining and the proportion of positive tumor cells were recorded. A staining index (with values 0–9) was calculated as the product of the staining intensity (0–3) and the area of positive staining (1, <10%; 2, 10–50%; 3, >50%).[22]

Statistical analysis. Statistical analyses such as the Student's *t*-test and the Pearson's correlation coefficient test were carried out using StatView (version 4.5, Abacus Concepts Inc, Piscataway, NJ, USA). A P-value of <0.05 was considered significant.

Results

Figure 1 shows that the cells stained positively for vasohibin, VEGFR-2, CD34, and D2-40 on the normal cervix, CIS, SCC, and Adenocarcinoma. There were no significant differences between clinical factor (lymph node metastasis, vessel involvement, parametrium invasion) and MVD, LVD, the vasohibin expression ratio in the microvessels, the VEGFR-2 expression ratio in the microvessels, and the histology score of VEGF-A expression.

Microvessel density. CD34-positive MVD (number of vessels per mm^2) were: 34.7 ± 2.5 in normal cervical epithelium; 46.1 ± 2.5 in CIS; 45.7 ± 3.5 in SCC; and 73.85 ± 8.4 in Adenocarcinoma (Fig. 2A). The MVD of Adenocarcinoma was significantly higher than that of the normal cervical epithelium, CIS and SCC. The MVD of normal cervical epithelium was significantly lower than that of CIS and SCC.

Lymphatic vessel density. D2-40-positive LVD (number of vessels per mm^2) was: 3.7 ± 0.8 in the normal cervical epithelium; 7.3 ± 0.8 in CIS; 17.6 ± 1.8 in SCC; and 34.6 ± 6.5 in Adenocarcinoma (Fig. 2B). The LVD of Adenocarcinoma was significantly higher than that of the normal cervical epithelium, CIS, and SCC. The LVD of SCC was significantly higher than that of the normal cervical epithelium and CIS. The LVD of CIS was significantly higher than that of the normal cervical epithelium.

Vasohibin expression ratio in microvessels. The positive ratio of vasohibin in microvessels was 53.6 ± 4.2% in normal cervical epithelium; 59.1 ± 4.6% in CIS; 71.5 ± 3.2% in SCC; and 79.3 ± 4.0% in Adenocarcinoma (Fig. 2C). The vasohibin-immunopositivity of the Adenocarcinoma microvessels was significantly higher than that of the normal cervical epithelium, CIS, and SCC. The vasohibin-immunopositivity of the SCC microvessels was significantly higher than that of the normal cervical epithelium and CIS.

VEGFR-2 expression in microvessels. The positive ratio of VEGFR-2 in microvessels was 42.6 ± 3.8% in the normal cervical epithelium; 42.1 ± 4.3% in CIS; 52.6 ± 2.6% in SCC; and 58.2 ± 4.7% in adenocarcinoma (Fig. 2D). The VEGFR-2 immunopositivity in Adenocarcinoma microvessels was significantly higher than that of the normal cervical epithelium, CIS, and SCC. The VEGFR-2 immunopositivity of SCC microvessels was significantly higher than that of the normal cervical epithelium and CIS.

Histology score of VEGF-A expression. VEGF-A expression was present in the cytoplasm of epithelial cells. The VEGF-A

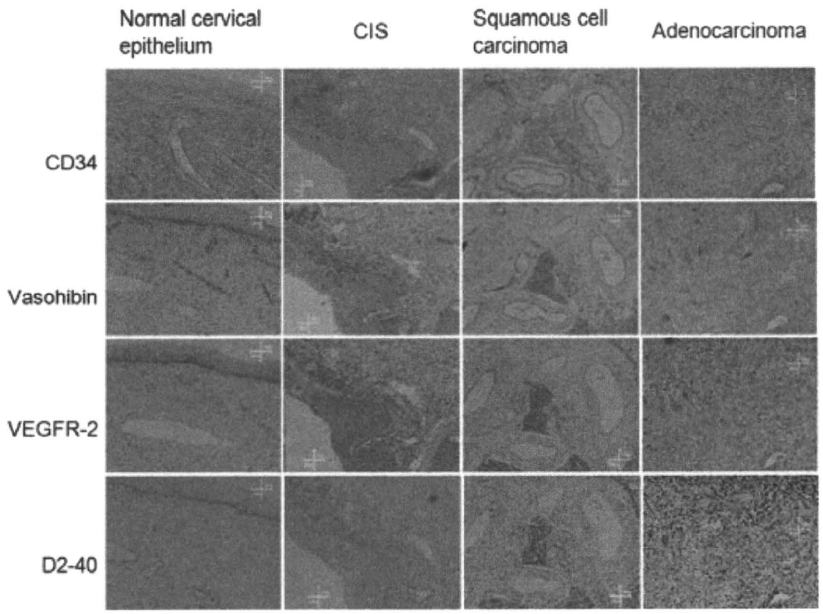

Fig. 1. Immunohistochemistry of the normal cervix with a normal epithelium, carcinoma *in situ* (CIS), squamous cell carcinoma, and adenocarcinoma. All sections are positively stained for: vasohibin (upper left, original magnification, ×200); vascular endothelial growth factor receptor-2 (VEGFR-2; upper right, original magnification, ×200); CD34 (lower left, original magnification, ×200; lower right, original magnification, ×400); and D2-40 (lower right, original magnification, ×200).

positive ratio of cytoplasmic staining intensity was: 37.9 ± 7.3 in the normal squamous epithelium; 58.6 ± 9.1 in CIS; 88.5 ± 8.7 in SCC; and 52.8 ± 16.3 in Adenocarcinoma (Fig. 2E). The VEGF-A positive ratio of cytoplasmic staining intensity in SCC was significantly higher than that of the normal squamous epithelium, CIS, and Adenocarcinoma. The VEGF-A positive ratio of cytoplasmic staining intensity in CIS was significantly higher than that of the normal squamous epithelium.

Correlation between vasohibin and VEGFR-2 positive ratios in microvessels. We emphatically analyzed through normal cervix–CIS–SCC as the multi-step carcinogenesis model. A moderate positive correlation existed between vasohibin and VEGFR-2 positive ratios in the microvessels of the normal cervical epithelium, CIS, and SCC ($P < 0.05$, $r^2 = 0.301$) (Fig. 3).

Discussion

Using immunohistochemistry, we examined the vascular density of cervical cancer and compared it with that of the normal cervix. Our results with MVD and LVD in CIS and SCC were almost identical with some previous reports.[3–5,23] Therefore, this proved the validity of our investigation. The major common perception of cervical cancer is that a CIS integrates the human papillomavirus and progresses to SCC in several years. Some reports indicate that the MVDs of CIS and SCC are greater than the MVD of the normal cervix. Therefore, we thought that it was important in our investigation to consider the vessel number in the normal cervix and to compare it with that of CIS and SCC. In accordance with our expectation, the MVD and LVD in the normal cervix were significantly lower than in CIS and SCC. These results suggested that hypervascularity is an important phenomenon of the progression of cervical squamous neoplasia. One published report showed that the VEGF intensity of SCC of the cervix increases in correlation with the clinical stage;[24] however, in the study there was no significance between the clinical features and the MVD, LVD, vasohibin expression ratio, VEGFR-2 expression ratio, and histological score (H score) of VEGF-A. In our study, we only found significant histological differences in the normal cervix, CIS, SCC, and Adenocarcinoma. Of course, it is important to investigate more cases of cervical neoplasia, and we suggest that peritumoral stromal angiogenesis is strongly ruled by the histological type of tumor. The VEGF-A positive ratio of cytoplasmic staining intensity in the normal cervical epithelium was significantly lower than that in CIS and in SCC. This result clearly showed that the cytoplasmic expression level of VEGF-A in squamous epithelium cells and squamous neoplasia was increased in accordance with the progression.

It is generally accepted that, at the same clinical stage, Adenocarcinoma has a poorer prognosis than SCC.[25–29] However, angiogenesis in Adenocarcinoma has been analyzed relatively little because of the minor frequency of Adenocarcinoma. In this study, we compared normal cervix, CIS, SCC, and Adenocarcinoma. We clearly showed that MVD and LVD were significantly higher in Adenocarcinoma than in SCC. This finding might contribute to understanding the poorer prognosis of adenocarcinoma of the cervix. To our regret, in this study we did not establish the significance between LVD and lymph node metastasis, because of insufficient number of cases. To clarify the issue, the same investigation should be repeated in a higher number of cases. However, the H score of VEGF-A of Adenocarcinoma was lower than that of SCC. We believe that it was difficult to detect VEGF-A in the cytoplasm of Adenocarcinoma because the cytoplasm was rich in mucus. In an *in vitro* study, there are many methods of measuring proteins in the cytoplasm, so we must examine measuring proteins in paraffin-embedded tissues except immunohistochemistry. Similar to MVD, LVD in this study was significantly increased in SCC and Adenocarcinoma. Some studies have reported the presence of peritumoral lymphatic vessels in cervical cancers and show that a high LVD is strongly associated with aggressive cervical cancer features such as lymph node metastasis, vessel involvement, parametrium invasion, and poor prognosis.[30,31] Although we expected that the LVD would be correlated with lymph node metastasis, there was no significant correlation between the two.

We examined the expression of vasohibin, as described in our previous report.[16] Vasohibin is induced in ECs by stimulation with VEGF.[12,15] Indeed, the expression of vasohibin in tumor vessels was shown to be correlated with that of VEGF in human breast cancer and human non-small cell lung carcinoma.[17,18] However, because of the difficulty of immunostaining VEGF-A in adenocarcinoma, we did not show such correlation in this study. VEGFR-2 receptor transduces most of the angiogenesis-related signals in ECs. The VEGF/VEGFR-2 signaling pathway is also important for the induction of vasohibin in Ecs.[15] We previously revealed that the VEGF-A-mediated induction of

doi: 10.1111/j.1349-7006.2010.01812.x

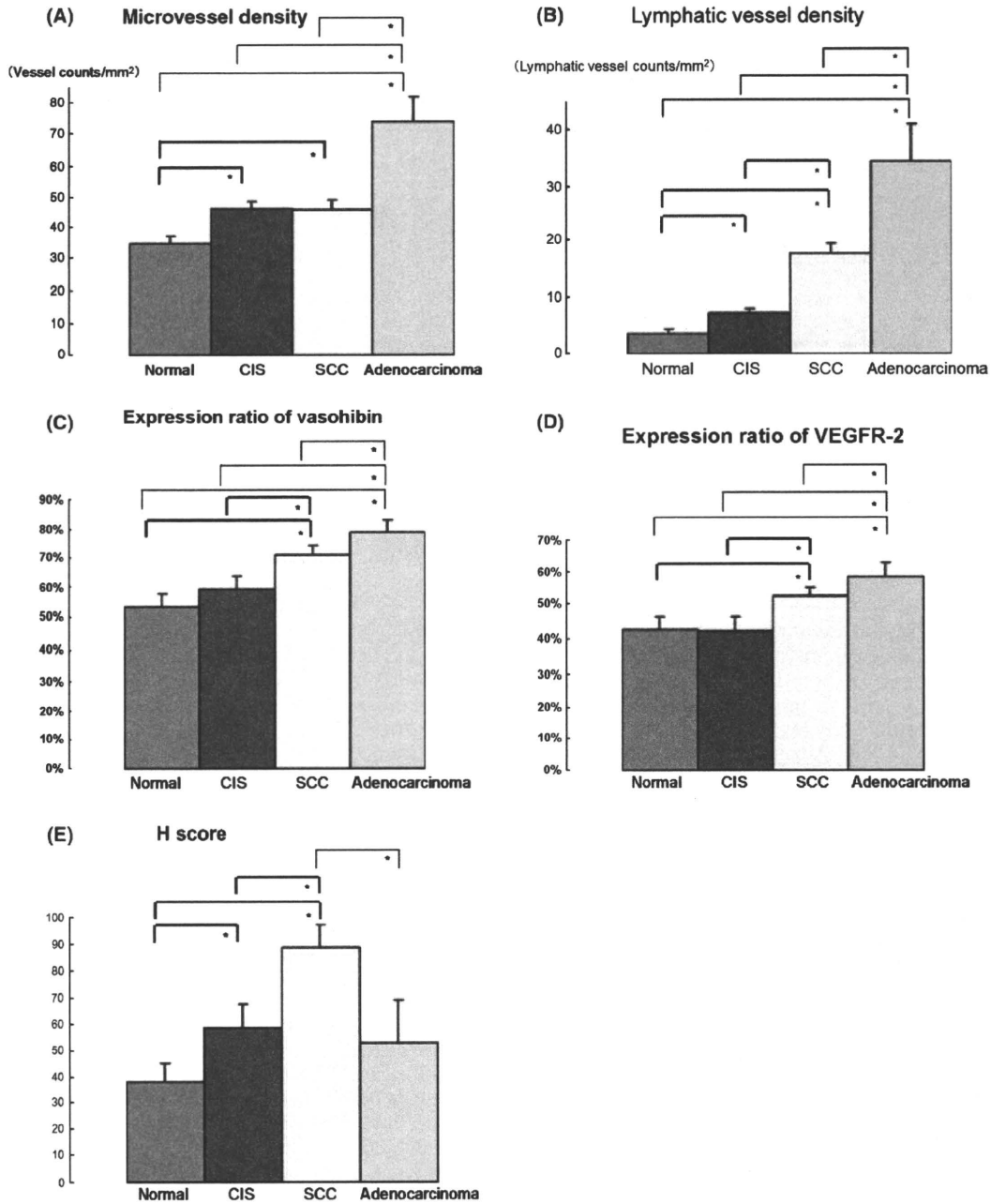

Fig. 2. (A) Microvessel density (MVD) of the normal cervix, carcinoma *in situ* (CIS), squamous cell carcinoma (SCC), and mucinous adenocarcinoma (Adenocarcinoma). The MVD of Adenocarcinoma is significantly higher than that of the normal cervix, CIS, and SCC. The MVD of the normal cervix is significantly lower than that of CIS and SCC. $*P < 0.05$. (B) Lymphatic vessel density (LVD) of the normal cervix, CIS, SCC, and Adenocarcinoma. The LVD of Adenocarcinoma is significantly higher than that of the normal cervix, CIS, and SCC. The LVD of SCC is significantly higher than that of the normal cervix and CIS. The LVD of CIS is significantly higher than that of the normal cervix. $*P < 0.05$. (C) The proportion of vasohibin/CD34-positive vessels in the normal cervix, CIS, SCC, and Adenocarcinoma. Vasohibin immunopositivity in microvessels in Adenocarcinoma is significantly higher than that in the normal cervix, CIS, and SCC. Vasohibin immunopositivity in the microvessels in SCC is significantly higher than that in the normal cervix and CIS. $*P < 0.05$. (D) Proportion of vascular endothelial growth factor receptor-2 (VEGFR-2)/CD34-positive vessels in the normal cervix, CIS, SCC, and Adenocarcinoma. VEGFR-2 immunopositivity in the microvessels in adenocarcinoma is significantly higher than in the normal cervix, CIS, and SCC. VEGFR-2 immunopositivity in the microvessels in SCC is significantly higher than in the normal cervix and CIS. $*P < 0.05$. (E) VEGF-A staining indexes of the cytoplasm of the tumor cell and normal cervical epithelium cells. The VEGF-A positive ratio of cytoplasmic staining intensity in SCC is significantly higher than that in the normal squamous epithelium, CIS, and Adenocarcinoma. The VEGF-A positive ratio of cytoplasmic staining intensity in CIS is significantly higher than in the normal squamous epithelium. H score, histological score. $*P < 0.05$.

vasohibin was preferentially mediated through the VEGFR-2 signaling pathway.[15] In our results, the expression ratio of vasohibin in vascular endothelial cells increased as the tissue progressed from a normal cervix to SCC to Adenocarcinoma. In addition, the expression ratio of VEGFR-2 in vascular endothelial cells increased as the tissue progressed from a normal cervix to SCC to Adenocarcinoma. This correlation of vasohibin and VEGFR-2 is also evident in endometrial adenocarcinoma[16] and

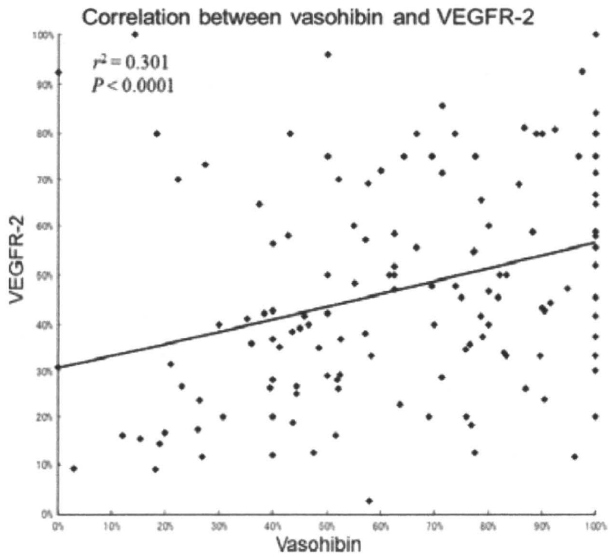

Fig. 3. Correlation between vasohibin and vascular endothelial growth factor receptor-2 (VEGFR-2). A moderate positive correlation exists between vasohibin-positive and VEGFR-2-positive ratios in the microvessels of the normal cervical epithelium, carcinoma *in situ*, and squamous cell carcinoma ($P < 0.0001$, $r^2 = 0.301$).

human breast cancer.[17] Thus, the pathological studies from human cancer specimens, including our present one, support the theory on the negative feedback role of vasobihin in cancers. Lu *et al.*[32] recently reported that the increased expression of Zeste homolog 2 (EZH2) predicts poor prognosis of ovarian cancers. This poor prognosis was explained by EZH2-mediated silencing of vasohibin expression in tumor vessels. As the level of vasohibin expression is considerably variable (Fig. 3), it would be interesting to see whether lower expression of vasohibin in tumor vessels predicts poor prognosis.

It has been established that there is a significant relationship between cervical papillomavirus infection and cervical cancer. It is also clear that CIS progresses to SCC in several years. In our study, a moderate positive correlation existed between the positive ratios of vasohibin and VEGFR-2 expression in the normal cervix, CIS, and SCC. As the expression of vasohibin increased in correlation with the expression of VEGFR-2, vasohibin could be an important biomarker of angiogenesis in the normal cervix and in cervical cancer. However, further investigations are required to clarify the precise role of vasohibin in regulating anti-angiogenic activity in the normal cervix and in cervical disorders.

We previously reported the function of vasohibin as a novel angiogenesis inhibitor.[12–15,18,33] The profiling of vasohibin expression in human cancer tissues is being accumulated.[18,33,34] In the future, vasohibin could potentially have medical application as a novel angiogenesis inhibitor.

Acknowledgments

The authors thank Miss Keiko Abe and Miss Emi Endo for preparing material. This work was supported by a Grant-in-Aid from the Kurokawa Cancer Research Foundation and a Grant-in-Aid for Scientific Research on Priority Areas from the Ministry of Education, Science and Culture, Japan and a Grant-in-Aid from the Ministry of Health, Labor and Welfare, Japan, and the 21st Century COE Program Special Research Grant (Tohoku University) from the Ministry of Education Science, Sports and Culture, Japan.

Disclosure Statement

The authors have no conflict of interest to declare.

Abbreviations

CIS	carcinoma *in situ*
EC	endothelial cell
SCC	squamous cell carcinoma
MVD	microvessel density
LVD	lymphatic vessel density
VEGF	vascular endothelial growth factor
VEGFR-2	VEGF receptor-2

References

1 American Cancer Society. Cancer Facts & Figures 2008. [Cited 21 May 2008.] Available from URL: http://www.cancer.org/downloads/STT/2008CAFFfinalsecured.pdf.
2 National Cancer Center Japan, 2001 (Website on the internet). Tokyo: National Cancer Center Japan, 2010. [Cited 1 Nov 2010.] Available from URL: http://ganjoho.jp/pro/statistics/en/gdball.html?1%2%1.
3 Obermair A, Bancher-Todesca D, Bilgi S, Kaider A, Kohlberger P. Correlation of vascular endothelial growth factor expression and microvessel density in cervical intraepithelial neoplasia. *J Natl Cancer Inst* 1997; **89**: 1212–7.
4 Dobbs S, Hewett P, Johnson I, Carmichael J, Murray J. Angiogenesis is associated with vascular endothelial growth factor expression in cervical intraepithelial neoplasia. *Br J Cancer* 1997; **76**: 1410–5.
5 Triratanachat S, Niruthisard S, Trivijitsilp P, Tresukosol D, Jarurak N. Angiogenesis in cervical intraepithelial neoplasia and early-staged uterine cervical squamous cell carcinoma: clinical significance. *Int J Gynecol Cancer* 2006; **16**: 575–80.
6 Cantu de leon D, Lopez-graniel C, Mendivil M. Significance of microvascular density (MVD) in cervical cancer recurrence. *Int J Gynecol Cancer* 2003; **13**: 856–62.
7 Loncaster JA, Cooper RA, Logue JP, Davidson SE, Hunter RD, West CM. Vascular endothelial growth factor (VEGF) expression is a prognostic factor for radiotherapy outcome in advanced carcinoma of the cervix. *Br J Cancer* 2000; **83**: 620–5.
8 Hammes LS, Tekmal RR, Naud P *et al.* Up-regulation of VEGF, c-fms and COX-2 expression correlates with severity of cervical cancer precursor (CIN) lesions and invasive disease. *Gynecol Oncol* 2008; **110**: 445–51.
9 Gombos Z, Xu X, Chu CS, Zhang PJ, Acs G. Peritumoral lymphatic vessel density and vascular endothelial growth factor C expression in early-stage squamous cell carcinoma of the uterine cervix. *Clin Cancer Res* 2005; **11**: 8364–71.
10 Gao P, Zhou GY, Yin G *et al.* Lymphatic vessel density as a prognostic indicator for patients with stage I cervical carcinoma. *Hum Pathol* 2006; **37**: 719–25.
11 Longatto-Filho A, Pinheiro C, Pereira SM *et al.* Lymphatic vessel density and epithelial D2-40 immunoreactivity in pre-invasive and invasive lesions of the uterine cervix. *Gynecol Oncol* 2007; **107**: 45–51.
12 Watanabe K, Hasegawa Y, Yamashita H *et al.* Vasohibin as an endotheliumderived negative feedback regulator of angiogenesis. *J Clin Invest* 2004; **114**: 898–907.
13 Sonoda H, Ohta H, Watanabe K, Yamashita H, Sato Y. Multiple processing forms and their biological activities of a novel angiogenesis inhibitor Vasohibin. *Biochem Biophys Res Commun* 2006; **342**: 640–6.
14 Shibuya M, Claesson-Welsh L. Signal transduction by VEGF receptors in regulation of angiogenesis and lymphangiogenesis. *Exp Cell Res* 2006; **312**: 549–60.
15 Shimizu K, Watanabe K, Yamashita H *et al.* Gene regulation of a novel angiogenesis inhibitor, Vasohibin, in endothelial cells. *Biochem Biophys Res Commun* 2005; **327**: 700–6.
16 Yoshinaga K, Ito K, Moriya T *et al.* Expression of vasohibin as a novel endothelium-derived angiogenesis inhibitor in endometrial cancer. *Cancer Sci* 2008; **99**: 914–9.
17 Tamaki K, Moriya T, Sato Y *et al.* Vasohibin-1 in human breast carcinoma: a potential negative feedback regulator of angiogenesis. *Cancer Sci* 2009; **100**: 88–94.
18 Hosaka T, Kimura H, Heishi T *et al.* Vasohibin-1 expression in endothelium of tumor blood vessels regulates angiogenesis. *Am J Pathol* 2009; **175**: 430–9.
19 Tavassoli FA, Devillee P. World Health Organization classification of tumours. In: Tavassoli FA, Devilee P, eds. *Pathology and Genetics of*

doi: 10.1111/j.1349-7006.2010.01812.x

Tumours of the Breast and Female Genital Organs. Lyon: IARC Press, 2003; 217–32.
20 Creasman WT. Announcement FIGO stages: 1988 revisions. *Gynecol Oncol* 1989; **35**: 125–7.
21 Weidner N, Semple JP, Welch WR, Folkman J. Tumor angiogenesis and metastasis correlation in invasive breast carcinoma. *N Engl J Med* 1991; **324**: 1–8.
22 Wagatsuma S, Konno R, Sato S, Yajima A. Tumor angiogenesis, hepatocyte growth factor, and c-Met expression in endometrial carcinoma. *Cancer* 1998; **82**: 520–30.
23 Randall LM, Monk BJ, Darcy KM *et al.* Markers of angiogenesis in high-risk, early-stage cervical cancer: a Gynecologic Oncology Group study. *Gynecol Oncol* 2009; **112**: 583–9.
24 Goncharuk IV, Vorobjova LI, Lukyanova NY, Chekhun VF. Vascular endothelial growth factor exression in uterine cervical cancer: correlation with clinicopathologic characteristics and survival. *Exp Oncol* 2009; **31**: 179–81.
25 Hopkins MP, Morley GW. A comparison of adenocarcinoma and squamous cell carcinoma of the cervix. *Obstet Gynecol* 1991; **77**: 912–7.
26 Hopkins MP, Schmidt RW, Roberts JA, Morley GW. The prognosis and treatment of stage I adenocarcinoma of the cervix. *Obstet Gynecol* 1988; **72**: 915–21.
27 Eifel PJ, Morris M, Oswald MJ, Wharton J T, Delclos L. Adenocarcinoma of the uterine cervix: prognosis and patterns of failure in 367 cases. *Cancer* 1990; **65**: 2507–14.
28 Eifel PJ, Burke TW, Morris M, Smith TL. Adenocarcinoma as an independent risk factor for disease recurrence in patients with stage IB cervical carcinoma. *Gynecol Oncol* 1995; **59**: 38–44.
29 Kleine W, Rau K, Schwoeorer D, Pfleiderer A. Prognosis of the adenocarcinoma of the cervix uteri: a comparative study. *Gynecol Oncol* 1989; **35**: 145–9.
30 Zhang SQ, Yu H, Zhang LL. Clinical implications of increased lymph vessel density in the lymphatic metastasis of early-stage invasive cervical carcinoma: a clinical immunohistochemical method study. *BMC Cancer* 2009; **9**: 64.
31 Botting SK, Fouad H, Elwell K *et al.* Prognostic significance of peritumoral lymphatic vessel density and vascular endothelial growth factor receptor 3 in invasive squamous cell cervical cancer. *Transl Oncol* 2010; **3**: 170–5.
32 Lu C, Han HD, Mangala LS *et al.* Regulation of tumor angiogenesis by EZH2. *Cancer Cell* 2010; **18**: 185–97.
33 Suzuki Y, Kobayashi M, Miyashita H, Ohta H, Sonoda H, Sato Y. Isolation of a small vasohibin-binding protein (SVBP) and its role in vasohibin secretion. *J Cell Sci* 2010; **123**: 3094–101.
34 Tamaki K, Sasano H, Maruo Y *et al.* Vasohibin-1 as a potential predictor of aggressive behavior of ductal carcinoma *in situ* of the breast. *Cancer Sci* 2010; **101**: 1051–8.

Pharmaceuticals **2011**, *4*, 782-793; doi:10.3390/ph4060782

OPEN ACCESS

pharmaceuticals

ISSN 1424-8247

www.mdpi.com/journal/pharmaceuticals

Article

Mutual Balance between Vasohibin-1 and Soluble VEGFR-1 in Endothelial Cells

Hiroki Miyashita [1], Hirotada Suzuki [1,2], Akihide Ohkuchi [2] and Yasufumi Sato [1,*]

[1] Department of Vascular Biology, Institute of Development Aging and Cancer, Tohoku University, 4-1 Seiryo-machi, Aoba-ku, Sendai 980-8575, Japan

[2] Department of Obstetrics and Gynecology, Jichi Medical University School of Medicine, Japan

* Author to whom correspondence should be addressed; E-Mail: y-sato@idac.tohoku.ac.jp; Tel.: +81-22-717-8528; Fax: +81-22-717-8533.

Received: 25 April 2011; in revised form: 23 May 2011/ Accepted: 30 May 2011 / Published: 31 May 2011

Abstract: Vasohibin-1 (VASH1) is a VEGF-inducible gene of endothelial cells (ECs) that acts as a negative feedback regulator of angiogenesis. To further characterize the function of VASH1, we transfected human VASH1 gene into the mouse EC line MS1, established stable VASH1 expressing clones, and determined gene alteration by cDNA microarray analysis. Among the various angiogenesis-related genes, vascular endothelial growth factor type 1 receptor (VEGFR-1) and its alternative spliced form, soluble VEGFR1 (sVEGFR-1), were found to be the most significantly down-regulated genes. Transient overexpression of VASH1 in human umbilical vein endothelial cells confirmed the down-regulation of VEGFR-1 and sVEGFR-1. sVEGFR-1 is a decoy receptor for VEGF and inhibits angiogenesis. Interestingly, when sVEGFR-1 was overexpressed in ECs, it inhibited the expression of VASH1 in turn. These results suggest that VASH1 and sVEGFR-1, two angiogenesis inhibitors, mutually balance their expressions in ECs.

Keywords: angiogenesis inhibitor; endothelial cell; VASH1; sVEGFR-1

1. Introduction

Angiogenesis, the formation of neovessels, is involved in both physiological and pathological conditions. Angiogenesis is regulated by a local balance between stimulators and inhibitors. Angiogenesis stimulators include vascular endothelial growth factor (VEGF), whereas angiogenesis inhibitors include

thrombospondins, pigment epithelium derived factor, angiostatin, endostatin, and so forth [1].

The VEGF family consists of five members; VEGF-A, VEGF-B, VEGF-C, VEGF-D, and placenta growth factor (PlGF). There are also three VEGF receptor (VEGFR) tyrosine kinases; VEGFR-1, VEGFR-2 and VEGFR-3. Members of the VEGF family show different affinities for the receptors. VEGFR-1 is able to bind VEGF-A, VEGF-B and PlGF. VEGFR-2 is activated primarily by VEGF-A, but cleaved forms of VEGF-C and VEGF-D can also activate VEGFR-2. VEGFR-3 is activated by VEGF-C and VEGF-D. Vascular endothelial cells (ECs) express mainly VEGFR-1 and VEGFR-2, whereas lymphatic ECs mainly express VEGFR-3 in adults. VEGFR-2 is the major mediator of VEGF-A driven responses for angiogenesis. The binding-affinity of VEGFR-1 for VEGF-A is one order of magnitude higher than that of VEGFR2, whereas the kinase activity of VEGFR-1 is about 10-fold weaker than that of VEGFR-2 [2]. *VEGFR-1 (-/-)* mice died in utero because of overgrowth of ECs, but mice lacking the tyrosine kinase domain of VEGFR-1 remain healthy and have a normal vasculature [3,4]. Thus, the ligand binding domain of VEGFR-1 are sufficient for normal vascular development in embryo, most likely by sequestering VEGF-A from VEGFR-2.

We recently isolated vasohibin-1 (VASH1) from VEGF-A inducible genes in ECs that inhibits migration and proliferation of ECs in culture, and exhibits anti-angiogenic activity *in vivo* [5]. The expression of VASH1 in ECs is induced not only by VEGF-A but also by fibroblast growth factor 2 (FGF-2), another potent angiogenic factor [5,6]. Thus, VASH1 is thought to be a negative-feedback regulator of angiogenesis. Immunohistochemical analysis revealed that VASH1 protein is expressed selectively in ECs in the developing human or mouse embryo, is reduced in expression in the post-neonate, but is induced in ECs at the site of angiogenesis [7]. Analysis of the spatiotemporal expression and function of VASH1 during angiogenesis revealed that VASH1 is expressed not in ECs at the sprouting front but in ECs of newly formed blood vessels behind the sprouting front where angiogenesis is terminated [8]. The expression of VASH1 is evident in various pathological processes such as cancers [9-13], atherosclerosis [14], age-dependent macular degeneration (AMD) [15], diabetic retinopathy [16], and so forth. Moreover, when applied exogenously, VASH1 shows anti-angiogenic activity under various pathological conditions such as in tumors, arterial intimal thickening and retinal neovascularization [9,14,17]. However, the molecular mechanisms underlying angiogenesis inhibition by VASH1 remain to be characterized. Here we intended to characterize the target genes of VASH1 in ECs. Using cDNA microarray analysis of stable VASH1 expressing EC clones, we identified both full-length and soluble forms of VEGFR-1 as the target genes of VASH1 in ECs.

2. Materials and Methods

2.1. Cells

MS1, an immortalized cell line with a SV40 large T antigen from mouse pancreatic ECs [18], was purchased from American Type Culture Collection (Manassas, VA, USA). The cells were cultured in αMEM (Invitrogen, Carlsbad, CA, USA) supplemented with 10% fetal bovine serum (FBS, JRHBiosciences, San Antonio, TX, USA). Human umbilical vein endothelial cells (HUVECs) were obtained from KURABO (Osaka, Japan) and were cultured on type I collagen-coated dishes (IWAKI,

Tokyo, Japan) containing endothelial basal medium-2 (EBM-2; Clonetics Corp., San Diego, CA, USA) supplemented with EC growth supplements and 2% FBS.

2.2. Establishment of VASH1 Expressing MS1 Clones

To improve the activity of transcription, we placed the CMV promoter of the pcDNA3.1/Hygro plasmid (Invitrogen) with the chicken β-actin promoter derived from pCALL2 [19]. This vector, pCALL2-pcDNA3.1/Hygro, was used for the transfection in this study. For the production of the VASH1 expression vector, the human VASH1 gene (5481 bp) containing the complete open reading frame (386 n.t.-1483 n.t.) [5] was cloned into the pCALL2-pcDNA3.1/Hygro vector at multiple cloning sites (Xho-I and Not-I). MS1 cells were transfected with the VASH1 expression vector by using Effectene transfection reagent (Qiagen, Valencia, CA, USA) according to the manufacturer's protocol. After the transfection, the cells were selected by hygromycin (500 μg/mL, Invitrogen). Following the selection, the cells were seeded at 0.3 cells per well in 96 well plates with 100 μL of culture medium in each well. The cells were later expanded into larger wells.

2.3. Gene Transfer in HUVECs

A replication-defective adenovirus vector encoding the human VASH1 (AdVASH1) or the β-gal gene (AdLacZ) was prepared as described previously [5]. The replication-defective adenovirus vector encoding the human VEGFR-1 gene (AdVEGFR-1) was a generous gift from Masabumi Shibuya (Tokyo Medical and Dental University). The HUVECs were infected with the adenovirus vectors at a multiplicity of infection (MOI) of 10 to 100. After the infection, RNAs and proteins were extracted at 24 and 36 hours, respectively.

2.4. Reverse Transcriptase-Polymerase Chain Reaction (RT-PCR)

Total RNA was extracted by the acid guanidinium-phenol-chloroform method using ISOGEN (Nippon Gene, Toyama, Japan). RT-PCR was performed by using a one step RT-PCR kit (Invitrogen) according to the manufacturer's instructions. The following primer pairs were synthesized and used for amplification: the respective sense (S) and the antisense (AS) primer pairs used were as follows: mouse and human VASH1, 5'- ATGGACCTGGCCAAGGAAAT-3' and 5'-CATCCTTCTTCCGGTC CTTG-3'; mouse VEGFR-1, 5'-GCGCATGACGGTCATAGAAG-3' and 5'-CAGGTGTGGCGCTT CCGAAT-3'; human VEGFR-1, 5'-ATGGTCAGCTACTGGGACAC-3' and 5'-GAATGACGAGCTC CCTTCCTT-3'; mouse sVEGFR-1, 5'-ACTCTCAGACCCCTGGAATC-3' and 5'-GATCCGAGAGA AAATGGCCT-3'; human sVEGFR-1, 5'-CATCACTCAGCGCATGGCAA-3' and 5'-CAGCCTTTTT GTTGCGTGC-3'; mouse and human G3PDH, 5′-ACCACAGTCCATGCCATCAC-3′ and 5′-TCCAC CACCCTGTTGCTGTA-3′. The PCR consisted of 27 cycles of 94 °C for 15 s, at 58 °C for 30 s, and finally at 68 °C for 30 s. The PCR products were electrophoresed through a 2% agarose gel containing 0.5 mg/mL ethidium bromide and visualized.

2.5. Western Blot Analysis

Western blot analysis was performed as described previously [20]. Briefly, extracted protein was separated by SDS-PAGE on a 7.5-10% separating gel and transferred to a Hybond-ECL membrane

(Amersham, Buckinghamshire, UK). The membrane was incubated with anti-human VASH1 monoclonal antibody (Ab) [5], anti-VEGFR-1 Ab (Santa Cruz Biotechnology, Inc., CA, USA), anti-sVEGFR-1 Ab (Zymed Lab., San Francisco, CA, USA), or anti-ß-actin Ab (Sigma, St. Louis, MO, USA) as the primary antibody according to the manufacturer's instructions. The signal was visualized by using horseradish peroxidase-conjugated secondary antibodies and enhanced chemiluminescence (Immobilon Western, Millipore, Billerica, MA, USA) with a LAS-1000 image analyzer (Fuji Film, Tokyo, Japan).

2.6. Cell Proliferation

Cells were inoculated at a density of 1×10^4 per well into 100 mm dishes, and cultured in 10% FCS/αMEM. After incubation for the desired period, the cells were counted with a hemocytometer.

2.7. Cell Migration

Cells were harvested with trypsin-EDTA, resuspended in 10% FCS/αMEM in a final volume of 100 μL, loaded (5×10^4 cells per well) into the upper chamber of a Transwell Polycarbonate Membrane (pore size: 8 μm; Costar, Cambridge, MA, USA) containing 600 μL of 10% FCS/αMEM in the lower chamber, and incubated at 37 °C for 4 hours. Cells on the lower surface were stained with the reagents from a Diff Quick kit (International Reagents, Kobe, Japan) and counted.

2.8. cDNA Microarray Analysis

Total RNA was isolated from the mock control and clone 4 by ISOGEN according to the manufacturer's instructions. The RNAs were reverse-transcribed in the presence of Cy3 or Cy5-labeled CTP, respectively. The labeled probes were hybridized to a Filgen Array Mouse 32K (Oxford Gene Technology, Oxford, UK) containing 31,769 genes, and the signals were detected by use of a GenePix 4000B (Olympus, Tokyo, Japan). Genes with a Cy5 signal/Cy3 signal ratio >2.0 or < 0.5 were considered to have changed in activity.

2.9. Blood Pressure and Urinary Albumin Excretion of Mice

Animal studies were reviewed and approved by the committee for animal study at our institute in accord with established standards of humane handling. AdVASH1, AdVEGFR-1 or AdLacZ (1×10^9 plaque-forming units [pfu]) was intravenously injected into a tail vein of BALB/c mice (Charles River Laboratories Japan, INC.). Before and seven days after the viral injection, mean blood pressure of conscious mice was measured by the tail cuff method (BP-98A; Softron Co. Ltd., Tokyo, Japan) according to the manufacture's instruction. Seven days after the viral injection, mice were put in mouse metabolic cages (Metabolica type MM; Sugiyama-Gen Iriki Co. Ltd., Tokyo, Japan) and urine was collected for successive eight hour periods. Urine was centrifuged at 2,000× *g* and the urinary albumin level was determined using an ELISA kit (Albuwell M; Exocell, Philadelphia, PA). Urinary creatinine levels were also measured by an ELISA kit (The Creatinine Companion; Exocell).

2.10. Calculations and Statistical Analysis

The statistical significance of differences in the data was evaluated by use of unpaired analysis of variance, and P values were calculated by the unpaired Student t test. $P < 0.05$ was accepted as statistically significant.

3. Results

We introduced the human VASH1 gene into MS1 cells, established bulk transfectants, and thereafter isolated 3 clones. First the expression of VASH1 mRNA and protein was determined (Figure 1A and B). We then examined the properties of the VASH1 expressing mouse endothelial clones. As expected, migration and proliferation were significantly decreased in these VASH1 transfectants (Figures 1C and D).

Figure 1. Establishment of VASH1 overexpressing MS1 clones.

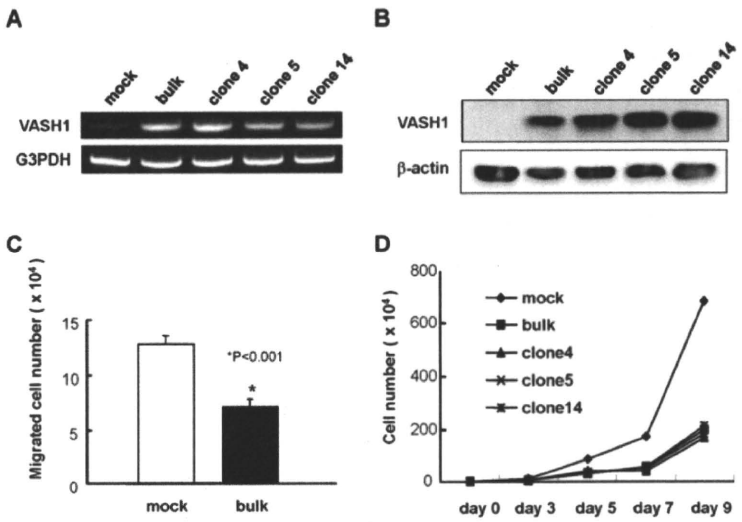

Establishment of VASH1 overexpressing MS1 bulk and clones was described in Materials and Methods. Total RNAs and proteins were extracted from each clone. RT-PCR (A) and Western (B) blot analysis for VASH1 was performed. (C) Migration was compared between mock and VASH1 transfectants. Means and SDs are shown. (D) Proliferation was compared between mock and VASH1 transfectants.

We used clone 4 (Figure 2A) for the following analysis, as it showed the highest expression of VASH1 (Figure 1A). Total RNA was isolated and the gene expression profile was compared with the mock control by cDNA microarray analysis (Figure 2B). The scatter plot of the mock control versus clone 4 is shown in Figure 2B. Among 31,769 mouse genes, 170 genes were increased by more than 200%, whereas 178 genes were decreased by less than 50% in clone 4. The top 20 up-regulated and down-regulated genes are listed in Table 1 and Table 2, respectively. We further evaluated the known angiogenesis-related genes. It was revealed that the expression of 7 genes (CCL2, CCL5, TIMP-1, COX-2, ARNT, CXCL1, and Jagged1) was augmented by more than 200%, whereas that of 2 genes (VEGFR-1 and Ets-1) was down-regulated by less than 50% (Table 3).

Figure 2. Scatter plot of mock vs. VASH1 over expression clone 4.

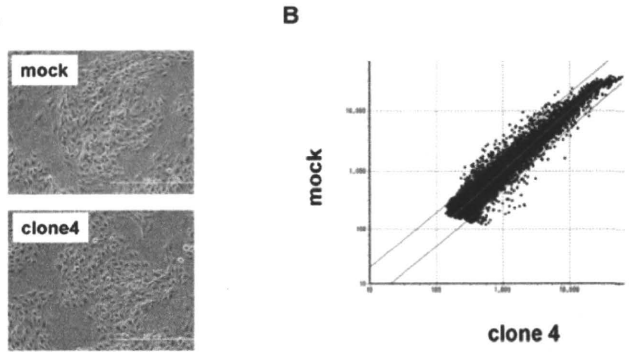

(A) Morphology of mock and VASH1 expressing clone 4 is shown. **(B)** RNAs were extracted from the mock and clone 4, and cDNA microarray analysis was performed as described in Materials and Method. Two lines indicate a 1:2 (lower) or 2:1 (upper) ratio between mock vs. VASH1 overexpressing clone 4.

Table 1. Top 20 up-regulated genes in the VASH1 stable transfectant.

Fold induction	Gene name	Accession No.
8.07	Estradiol 17 beta-dehydrogenase 5	NM_030611
7.65	T-cell specific GTPase	NM_011579
6.16	Dematin	NM_013514
5.43	interferon-induced protein with tetratricopeptide repeats 3	NM_010501
4.91	Osteoactivin	NM_053110
4.63	BTB/POZ domain containing protein 9	NM_172618
4.29	interferon, alpha-inducible protein	NM_172618
4.26	Galectin-3	NM_010705
4.19	ADP-ribosylation factor-like 2 binding protein	NM_024191
3.79	potassium channel interacting protein 4	NM_030265
3.79	CCL2	NM_011333
3.78	olfactory receptor 576	NM_001001805
3.59	KELCH-like protein 4	NM_172781
3.41	interferon-induced protein 44	NM_133871
3.39	interferon, alpha-inducible protein 27	NM_029803
3.12	acyl-Coenzyme A thioesterase 2	NM_019736
3.28	stefin A2 like 1	NM_173869
3.11	guanylate nucleotide binding protein 3	NM_018734
3.09	2'-5'-oligoadenylate synthetase 1A	NM_145211
3.00	Male-specific lethal 3-like 1	NM_010832

Table 2. Top 20 down-regulated genes in the VASH1 stable transfectant.

Fold induction	Gene name	Accession No.
0.22	Phospholipid transfer protein	NM_011125
0.22	VEGFR1	NM_010228
0.28	Oligodendrocyte transcription factor 1	NM_016968
0.28	olfactory receptor 635	NM_147118

Table 2. *Cont.*

0.28	PHD finger protein 19	NM_028716
0.28	Trace amine receptor 1	NM_053205
0.29	Gastrokine 1	NM_025466
0.29	Mast cell carboxypeptidase A	NM_007753
0.30	poliovirus receptor-related 2	NM_008990
0.30	Versican core protein	XM_488510
0.30	Janus kinase 3	NM_010589
0.30	thrombopoietin	NM_009379
0.31	nudix	NM_025539
0.31	Anaplastic lymphoma kinase	NM_007439
0.33	Lymphocyte antigen 86	NM_010745
0.33	Fc receptor-like 3	NM_144559
0.34	Serine/threonine-protein kinase ULK1	NM_009469
0.34	Runt-related transcription factor 3	NM_019732
0.34	RAB GTPase activating protein 1	AK_044346
0.35	kidney expressed gene 1	NM_029550

Table 3. Altered expression of angiogenesis-related genes in the VASH1 transfectant.

Gene name	**Fold induction**
VEGFR1	0.22
Ets-1	0.45
Jagged1	2.06
CXCL1	2.17
ARNT	2.18
COX-2	2.38
TIMP-1	2.39
CCL5	2.45
CCL2	3.79

Here we focused our attention on VEGFR-1, the most down-regulated gene. The characteristic feature of the VEGFR-1 gene is that it encodes not only a full-length membrane receptor but also a soluble form (sVEGFR-1) carrying the VEGF-binding domain as well as a 31-amino-acid stretch derived from an intron [22]. We therefore analyzed the expression of sVEGFR-1 as well. RT-PCR and Western blot analyses showed decrease expression of VEGFR-1 and sVEGFR-1 in all VASH1 expressing clones (Figures 3A and 3B). To further confirm these results, we transiently overexpressed VASH1 in HUVECs. RT-PCR and Western blot analyses also showed this decrease in the levels of VEGFR-1 and sVEGFR-1 (Figures 3C and D).

sVEGFR-1 is a decoy receptor and inhibits VEGF mediated signals. VASH1 is a VEGF-inducible angiogenesis inhibitor expressed in ECs. We therefore examined whether sVEGFR-1 affects the expression of VASH1 in ECs. To do so, we transiently overexpressed the sVEGFR-1 gene in HUVECs. RT-PCR and Western blot analyses demonstrated that sVEGFR-1 down-regulated the expression of VASH1 in HUVECs (Figure 4).

Figure 3. VASH1 inhibits VEGFR-1 and sVEGFR-1 expression in ECs.

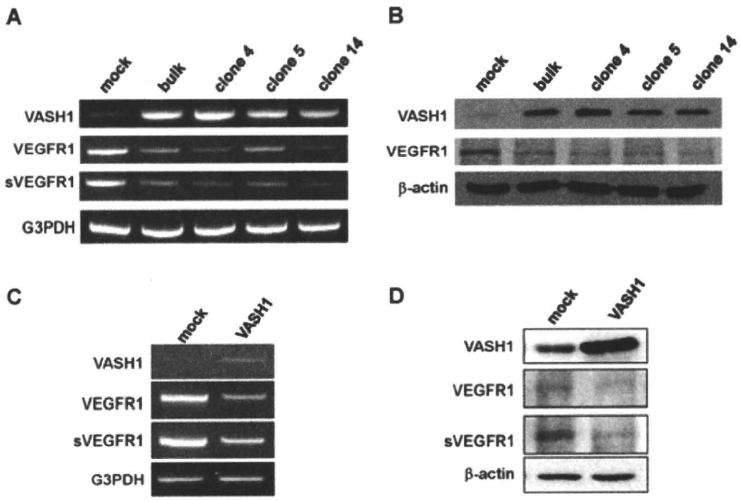

Total RNAs and proteins were extracted from mock cells and from each VASH1 overexpressing clone, and RT-PCR (A) and Western blot analysis (B) for VEGFR-1 and sVEGFR-1 were performed as described in Materials and Method. The HUVECs were infected with the Lac-Z or VASH1 adenovirus vector at a multiplicity of infection (MOI) of 30. After the infection, total RNAs and proteins were extracted from vasohibin-1 over expression HUVECs. RT-PCR (C) and Western (D) blot analysis for VEGFR-1 and sVEGFR-1 was performed.

Figure 4. sVEGFR-1 inhibits VASH1 expression in ECs.

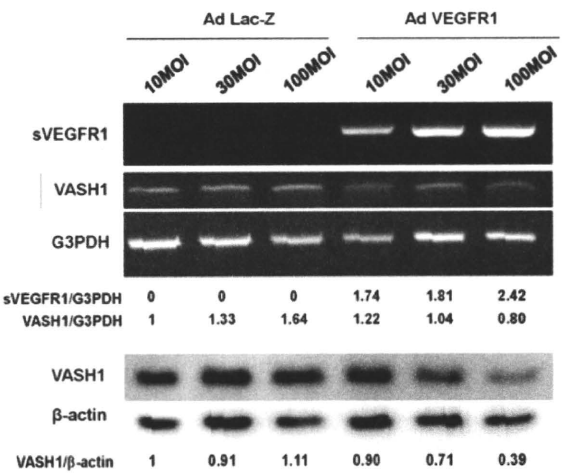

The HUVECs were infected with the AdsVEGFR-1 at the indicated a multiplicity of infection (MOIs). After the infection, total RNAs and proteins were extracted from sVEGFR-1 overexpressing HUVECs. RT-PCR (upper panel) and Western blot analysis (lower panel) for VASH1 were performed. Intensity of bands was quantified, and standardized values are shown.

The blockade of VEGF mediated signals causes regression of normal quiescent vessels, hypertension and proteinuria [21]. Here we examined whether VASH1 caused hypertension and proteinuria. AdsVEGFR-1 increased mean blood pressure, but AdVASH1 did not (Figure 5A). Similarly AdsVEGFR-1 increased the urinary albumin excretion, but AdVASH1 did not (Figure 5B).